Electronic Supporting Information

Biosynthesis of an anti-tuberculosis sesterterpenoid asperterpenoid A

Jia-Hua Huang,‡[a] Jian-Ming Lv,‡[a] Qiao-Zhen Wang,[a] Jian Zou,[a] Yong-Jun Lu,[b] Qing-Lin Wang,[b] Dong-Ni Chen,[c] Xin-Sheng Yao,[a] Hao Gao*[a] and Dan Hu*[a]

[a.] Institute of Traditional Chinese Medicine and Natural Products, College of Pharmacy / Guangdong Province Key Laboratory of Pharmacodynamic Constituents of TCM and New Drugs Research, Jinan University, Guangzhou 510632, People's Republic of China. Email: tghao@jnu.edu.cn; thudan@jnu.edu.cn

[b.] School of Life Sciences, Sun Yat-sen University, Guangzhou 510275, People's Republic of China

[c.] School of Marine Sciences, Sun Yat-sen University, Guangzhou 510275, People's Republic of China

Table of Contents

Supplementary Methods

General materials and experimental procedures

All the chemicals were purchased from Oceanpak Alexative Chemical Co., Ltd. (Gothenburg, Sweden) or Fine Chemical Co., Ltd. (Tianjin, China). The biochemical reagents and kits used in this work were purchased from TaKaRa Bio Inc. (Dalian, China), Thermo Fisher Scientific Inc. (Shenzhen, China) or Sangon Biotech Co., Ltd. (Shanghai, China), unless noted otherwise. Primer synthesis was performed by Sangon Biotech Co., Ltd. (Shanghai, China). PCR was carried out using a Mastercycler nexus gradient (Eppendorf, Hamburg, Germany) or an A100 Thermal cycler (LongGene, Hangzhou, China).

UV data, IR data and optical rotations were respectively measured on the JASCO V-550 UV/vis spectrometer, JASCO FT/IR-480 plus spectrometer, and JASCO P1020 digital polarimeter from JASCO International Co., Ltd. (Tokyo, Japan). The HRESIMS data were obtained on a Waters Micromass Q-TOF mass spectrometer (Milford, USA). 1D and 2D NMR spectra were recorded with the Bruker AV 600 spectrometer (Faellanden, Switzerland) using the solvent signals ($CDCl_3$: δ_H 7.26/δ_C 77.0; C_6D_6: δ_H 7.16/δ_C 128.1) as the reference. The semi-preparative HPLC was performed on an Ultimate 3000 HPLC system (Dionex) with a YMC-Pack ODS-A column (10.0 mm i.d. × 250 mm, 5 μm). The silica gel column chromatography was performed with silica gel (200-300 mesh, Haiyang Chemical Co., Ltd., Qingdao, China). The medium-pressure liquid chromatography (MPLC) was carried out using a dual-pump gradient system (Lisui E-Tech Co., Ltd., Shanghai, China) with ODS (50 μm, YMC Co., Ltd., Tokyo, Japan).

Strains and media

Talaromyces wortmannii ATCC 26942 purchased from the American Type Culture Collection (ATCC) was cultured in potato dextrose broth for DNA extraction. The quadruple auxotrophic host *Aspergillus oryzae* NSAR1 (*niaD*$^-$, *sC*$^-$, Δ*argB*, *adeA*$^-$)[1] was used for heterologous express of target genes under the *amyB* promoter in the modified Czapek-Dox (CD) medium (0.3% $NaNO_3$, 0.2% KCl, 0.05% $MgSO_4 \cdot 7H_2O$, 0.1% KH_2PO_4, 0.002% $FeSO_4 \cdot 7H_2O$, 1% polypeptone, 2% starch, pH 5.5). *Escherichia coli* DH5α (TaKaRa) strains carrying recombinant plasmids were grown in LB medium with appropriate antibiotics.

Genome sequencing of *T. wortmannii* ATCC 26942 and analysis

The whole genome of *T. wortmannii* ATCC 26942 was sequenced using an Illumina HiSeq 2500 system by Novogene Co., Ltd (Beijing, China). The raw data were assembled into contigs by the SOAPdenovo (http://soap.genomics.org.cn/soapdenovo.html). Gene prediction was performed with AUGUSTUS (http://bioinf.uni-greifswald.de/augustus/). All the predicted enzymes were used to construct the database for the local BLAST search.

Construction of recombinant plasmids

astA, *astB*, and *astC* were amplified from the genomic DNA of *T. wortmannii* ATCC 26942, and inserted into the linearized vector pTAex3 using T4 DNA ligase or ClonExpress® II One Step Cloning Kit (Vazyme, Nanjing, China) to yield pTAex3-*astA*, pTAex3-*astB*, and pTAex3-*astC*, respectively. Then DNA fragments containing the promoter and terminator amplified from the recombinant pTAex3 plasmids were cloned into the *Xba*I-digested pAdeA vector to afford pAdeA-*astA*, pAdeA-*astB*, and pAdeA-*astA*-*astB*. All the primers and plasmids used in this work are listed in Table S1 and S2.

Transformation of *A. oryzae* NSAR1

PEG-mediated protoplast transformation was employed to construct the *A. oryzae* transformant strain. 100 μL spore suspension of the parent strain was inoculated in 10 mL DPY medium (2% dextrin, 1% polypeptone, 0.5% yeast extract, 0.05% $MgSO_4 \cdot 7H_2O$, 0.5% KH_2PO_4) and cultivated for 1-2 days. Then the culture broth was transferred into 100 mL DPY. After growth for 1 day, mycelia were harvested, and the cell walls were removed using the Yatalase enzyme system (1% Yatalase, 0.6 M $(NH_4)_2SO_4$, 50 mM maleic acid, pH 5.5) at 30 ^oC for 3 hours. The protoplasts were collected and washed with Solution 2 (1.2 M sorbitol, 50 mM $CaCl_2 \cdot 2H_2O$, 35 mM NaCl, 10 mM Tris-HCl, pH 7.5), and then adjusted to around 1.0×10^7 mL^{-1} with Solution 2. 10 μg plasmids (~ 10 μL) and 200 μL protoplast suspension were gently mixed and placed on ice for 30 min. Subsequently, 1.35 mL PEG solution (60% PEG4000, 50 mM $CaCl_2 \cdot 2H_2O$, 10 mM Tris-HCl, pH 7.5) was added. After 20 min at the room temperature, 7 mL Solution 2 was added, and the mixture was subjected to centrifugation at 1500 rpm for 10 min. The precipitate was resuspended in 200 μL Solution 2, and spread on the under-layer medium, which was covered with the upper-layer medium. The selective medium contains 0.2% NH_4Cl, 0.1% $(NH_4)_2SO_4$, 0.05% KCl, 0.05% NaCl, 0.1% KH_2PO_4, 0.05% $MgSO_4 \cdot 7H_2O$, 0.002% $FeSO_4 \cdot 7H_2O$, 2% glucose, 1.2 M sorbitol and 0.8-1.5% agar as well as appropriate

ingredients for complementing auxotrophy. And the transformants could be obtained after incubation at 28 °C for 3-5 days and confirmed via PCR (Fig. S1).

Analysis of metabolites from *A. oryzae* transformants

The spore suspension of the *A. oryzae* transformant was inoculated into 10 mL DPY medium and was cultured at 28 °C and 200 rpm for 2 days as the seed broth. Then the broth was transferred into 100 mL modified CD medium for the induction of genes. After growth at 28 °C and 200 rpm for 6 days, the mycelia were harvested by filtration and extracted with acetone. The extract was dried under reduced pressure, and then partitioned with hexane-water (1/1, v/v) for GC-MS analysis, or resuspended in methanol for HPLC analysis.

GC-MS analysis was performed on Agilent Technologies 7890B GC System coupled with 5977B MSD using an HP-5MS 30 Meter column (0.32 mm i.d., 0.25 μm film thickness). The temperature of the ionization chamber was 230 °C, along with the electron impact ionization voltage of 70 eV. The oven temperature initially kept at 50 °C for 3 min, and then increased to 70 °C at a rate of 20 °C min^{-1} and held for 1 min, followed by a second ramp from 70 °C to 300 °C at a rate of 15 °C min^{-1} and holding for 3 min. Helium was used as carrier gas at the rate of 1 mL min^{-1}.

HPLC profile was detected on an Ultimate 3000 HPLC system (Dionex) using a COSMOSIL 3C_{18}-EB column (4.6 mm i.d. × 150 mm, 3 μm) with a linear gradient of 50-100% H_2O (0.1% formic acid)-CH_3CN (0.1% formic acid) in 25 min followed by 100% CH_3CN (0.1% formic acid) for 35 min at 1 mL min^{-1}.

Purification procedure for each metabolite

Mycelia from 2 L culture of the *A. oryzae* NSAR1 transformant harboring *astC* were extracted with acetone at room temperature. Then the extract (0.68 g) was subjected to silica gel column chromatography with cyclohexane to yield 89.5 mg of **1**.

Mycelia from 4 L culture of the *A. oryzae* NSAR1 transformant harboring *astB* and *astC* were extracted with acetone at room temperature. Then the extract (1.7 g) was subjected to silica gel column chromatography and MPLC with stepwise elution in order. Subfraction containing **2** and **3** was further purified by semi-preparative HPLC (YMC-Pack ODS-A column, 3 mL min^{-1}) with isocratic elution of 85% CH_3CN-H_2O containing 0.1% formic acid to yield **3** (t_R: 21.0 min, 3.0 mg) and **2** (t_R: 26.3 min, 15.0 mg).

Mycelia from 5 L culture of the *A. oryzae* NSAR1 transformant harboring *astA*, *astB*, and *astC* were extracted with acetone at room temperature. Then the extract (1.4 g) was subjected to silica gel column chromatography and MPLC with stepwise elution in order. Subfraction containing **4** was further purified by semi-preparative HPLC (YMC-Pack ODS-A column, 3 mL min^{-1}) with isocratic elution of 80% CH_3CN-H_2O containing 0.1% formic acid to yield **4** (t_R: 11.7 min, 25.0 mg).

Conformational analysis and quantum chemical ^{13}C NMR calculations of 4

The molecules of (6*S**, 7*R**, 9*R**, 10*S**, 11*S**, 14*S**, 15*S**, 16*R**, 18*R**)–**4A** and (6*S**, 7*R**, 9*R**, 10*S**, 11*S**, 14*S**, 15*S**, 16*R**, 18*S**)–**4B** were converted into SMILES codes before their initial 3D structures were generated with CORINA version 3.4. Conformer databases were generated in CONFLEX version 7.0 by using the MMFF94s force-field with an energy window for acceptable conformers (ewindow) of 5 kcal mol^{-1} above the ground state, a maximum number of conformations per molecule (maxconfs) of 100, and an RMSD cutoff (rmsd) of 0.5Å. Then each acceptable conformers was optimized with HF/6-31G(d) method in Gaussian09.[2] Further optimization at the B3LYP/6-31G(d) level determined the dihedral angles. From this, (11 for **4A** and 12 for **4B**) most stable conformers were determined (Table S6 and Fig. S6). The optimized conformers (11 for **4A** and 12 for **4B**) were used for ^{13}C NMR calculations, which were performed with Gaussian09 (B3LYP/6-31+G(d, p)). The solvent effects were taken into account by the polarizable-conductor calculation model (PCM, chloroform as the solvent). The comparison was judged by DP4+ probability.[3]

Heterologous expression, purification and inhibition assay for MptpB

The coding sequence of MptpB was amplified from the genomic DNA of *M. tuberculosis* H37Ra, and then cloned into the expression vector pET28a. Subsequently, the resulting recombinant vector was transformed into *E. coli* BL21(DE3). The transformant was grown in LB medium supplemented with 50 mg L^{-1} kanamycin at 37 °C until OD_{600} reached 0.6-0.8. The gene expression was induced with 0.1 mM isopropyl β-D-thiogalactopyranoside (IPTG) at 18 °C for 16 hours. The cells were harvested by centrifugation at 5000 × *g* for 5 min at 4 °C, and then resuspended in lysis buffer with 0.01% Triton X-100, 5 mL DTT and EDTA-free protease inhibitors cocktail, followed by sonication on ice. After centrifugation at 10000 × *g* for 30 min at 4 °C, the supernatant was collected and subjected to a Ni^{2+}-NTA affinity column. After

elution with washing buffer (25 mM Tris, 500 mM NaCl, 50 mM imidazole, pH 7.8) to remove the non-specific binding proteins, MptpB was eluted with elution buffer (25 mM Tris, 500 mM NaCl, 350 mM imidazole, pH 7.8). The eluate was concentrated and exchanged with the buffer (25 mM Tris, 100 mM NaCl, pH 7.8) using the Amicon Ultra centrifugal filter. MptpB was analyzed by 10% sodium dodecyl sulfate (SDS)-polyacrylamide gel electrophoresis (PAGE) and its content was determined by Bradford protein assay (Bio-Rad, USA). The purified MptpB was stored at -20 ^{o}C.

The phosphatase activity assay of MptpB was performed in triplicate in 96-well microplate in reaction buffer (50 mM Tris, 100 mM NaCl, pH 7.0) using *p*-nitrophenyl phosphate (*p*NPP) as a substrate. The MptpB inhibition was evaluated in a reaction mixture (final volume, 200 μL) containing 1.5 μg MptpB and 50 μM sample, and sodium orthovanadate was tested as the positive control. The reaction mixture was incubated for 10 min at room temperature, followed by addition of *p*NPP to a final concentration of 1.3 mM. The absorbance at 405 nm was measured in the spectrophotometer Infinite 200 PRO (TECAN). The negative control without MptpB was performed to account for the spontaneous hydrolysis of *p*NPP.

IC_{50} with more than 60% of inhibitory activity against MptpB was determined at 0.195-100 μM using two-fold dilution. The data were calculated by fitting the inhibition percentage and inhibitor concentration with Origin 9. Different inhibitor concentrations and different concentrations of *p*NPP were employed to determine the type of inhibition by fitting data to Lineweaver-Burk plot. All assays were performed in triplicate in at least three independent experiments.

Structural characterization

Preasperterpenoid A (**1**): A white powder; [α]31 *D* = +100.0 (*c* 1.5, $CHCl_3$); NMR spectra see Fig. S11 and S12; ^{1}H NMR (600 MHz, C_6D_6) δ_H 2.50 (m, 1H), 2.48 (d, *J* = 13.6 Hz, 1H), 2.44 (m, 1H), 2.11 (m, 1H), 2.09 (m, 1H), 1.98 (br dd, *J* = 12.6, 7.2 Hz, 1H), 1.88 (m, 1H), 1.86 (m, 1H), 1.70 (m, 2H), 1.66 (m, 1H), 1.65 (s, 3H), 1.54 (m, 1H), 1.52 (m, 1H), 1.44 (m, 1H), 1.39 (m, 1H), 1.33 (m, 1H), 1.29 (t, *J* = 10.8 Hz, 1H), 1.22 (dd, *J* = 11.4, 9.6 Hz, 1H), 1.10 (m, 1H), 1.00 (d, *J* = 6.8 Hz, 3H), 0.99 (s, 3H), 0.93 (s, 3H), 0.88 (d, *J* = 6.8 Hz, 3H), 0.79 (s, 3H), 0.60 (dd, *J* = 8.4, 4.2 Hz, 1H), 0.33 (t, *J* = 4.8 Hz, 1H), 0.19 (ddd, *J* = 9.6, 8.4, 5.4 Hz, 1H); ^{13}C NMR (150 MHz, C_6D_6) δ_C 136.2, 131.4, 54.7, 51.6, 47.8, 47.6, 45.8, 43.3, 40.5, 39.8, 39.7,

38.3, 36.5, 30.0, 28.9, 26.6, 25.2, 23.5, 23.0, 22.7, 21.0, 20.6, 17.9, 15.4, 13.7; The NMR data are in good agreement with those of preasperterpenoid A.[4]

Asperterpenoid A (**2**): A white powder; [α]32 D = +81.7 (c 1.0, $CHCl_3$); HRESIMS (positive) *m/z* 387.2903 $[M + H]^+$ (calcd for $C_{25}H_{39}O_3$, 387.2899), see Fig. S13; NMR spectra see Fig. S14-S19; NMR data are slightly different from the reported values of asperterpenoid A (Table S3).[5]

Asperterpenoid B (**3**): A white powder; [α]33 D = +70.5 (c 0.2, $CHCl_3$); UV ($CHCl_3$) λ_{max} (log ε) 242 (4.15); IR (KBr) ν_{max} 3444, 2954, 2864, 1687, 1637, 1403, 1091 cm^{-1}; HRESIMS (positive) *m/z* 801.5319 $[2M + H]^+$ (calcd for $C_{50}H_{73}O_8$, 801.5305), see Fig. S20; NMR spectra see Fig. S21-S26; NMR data see Table S4. **3** is identified as asperterpenoid B.

Asperterpenoid C (**4**): A white powder; [α]32 D = +37.0 (c 1.0, $CHCl_3$); UV ($CHCl_3$) λ_{max} (log ε) 243 (4.34); IR (KBr) ν_{max} 3552, 3412, 2946, 2866, 1688, 1644, 1397, 1257, 1097, 1047 cm^{-1}; HRESIMS (positive) *m/z* 403.2847 $[M + H]^+$ (calcd for $C_{25}H_{39}O_4$, 403.2848), see Fig. S27; NMR spectra see Fig. S28-S33; NMR data see Table S5. **4** is identified as asperterpenoid C.

Supplementary Tables

Table S1. Primers used for constructing recombinant plasmids

Primer	Sequence (5′ to 3′)	Usage
Infusion-*astA*-F	TCGAGCTCGGTACCCATGGAGCAGAGGGAAATTAT	Cloning of *astA* from *T. wortmannii* ATCC 26942 genome
Infusion-*astA*-R	CTACTACAGATCCCCTTAAGCACGAACCTCTAACC	
Infusion-*astB*-F	TCGAGCTCGGTACCCATGATCGACTCTTTGTCGTT	Cloning of *astB* from *T. wortmannii* ATCC 26942 genome
Infusion-*astB*-R	CTACTACAGATCCCCCACACAATTACTCAGTGACT	
astC-EcoRI-F	CCGGAATTCATGGCTTCTCTAGAGGTATT	Cloning of *astC* from *T. wortmannii* ATCC 26942 genome
astC-EcoRI-R	CCGGAATTCAAGTCTACTTCACATGCAAC	
Inf-pAdeA-Parm-F	GCAGGTCGACTCTAGACGACTCCAATCTTCAAGAGC	Construction of recombinant pAdeA plasmids containing one or two genes
Inf-pTAex3-Tamy-R_1	AACGCGCTCGCGAGCAAGTACCATACAGTACCGCG	
Inf-pTAex3-Parm-F_1	GCTCGCGAGCGCGTTCCACTGCATCATCAGTCTAG	
Inf-pAdeA-Tamy-R	TAGTAGATCCTCTAGAGTAAGATACATGAGCTTCGG	
astA-F	ATGGAGCAGAGGGAAATTAT	Cloning of *astA* from transformants
astA-R	TTAAGCACGAACCTCTAACC	
astB-F	ATGATCGACTCTTTGTCGTT	Cloning of *astB* from transformants
astB-R	TCAGTGACTTTGATCCGGAT	
astC-F	ATGGCTTCTCTAGAGGTATT	Cloning of *astC* from transformants
astC-R	AAGTCTACTTCACATGCAAC	

Table S2. Plasmids used in the study

Plasmid	Characteristic	Source
pTAex3	Plasmid containing *argB* maker gene cassette for gene expression in *A. oryzae* NSAR1. (Amp^R)	Fujii, T. *et al*.[6]
pAdeA	Plasmid containing *adeA* maker gene cassette for gene expression in *A. oryzae* NSAR1. (Amp^R)	Jin, F. *et al*.[7]
pTAex3-*astA*	pTAex3 containing *astA* under the *amyB* promoter. (Amp^R)	This work
pTAex3-*astB*	pTAex3 containing *astB* under the *amyB* promoter. (Amp^R)	This work
pTAex3-*astC*	pTAex3 containing *astC* under the *amyB* promoter. (Amp^R)	This work
pAdeA-*astA*	pAdeA containing *astA* under the *amyB* promoter. (Amp^R)	This work
pAdeA-*astB*	pAdeA containing *astB* under the *amyB* promoter. (Amp^R)	This work
pAdeA-*astA*-*astB*	pAdeA containing *astA* and *astB* under the *amyB* promoter. (Amp^R)	This work

Table S3. NMR assignments for 2 (^{1}H for 600 MHz and ^{13}C for 150 MHz in $CDCl_3$)

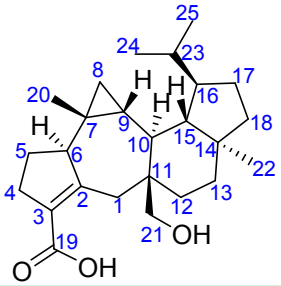

No.	δ_C, type	δ_H (J in Hz)[a]	^{1}H–^{1}H COSY	HMBC	ROESY
1	43.0, CH_2	a: 3.49, d (13.2)	1b	2, 3, 6, 10, 11, 12	12a
		b: 1.60, d (13.2)	1a	2, 3, 6, 10, 11, 21	6, 10, 12b
2	160.6, C				
3	127.5, C				
4	32.9, CH_2	2.60	5a, 5b	2, 3, 5, 6	20
5	26.0, CH_2	a: 2.02	4, 5b, 6	2, 3, 4, 6, 7	20
		b: 1.96	4, 5a, 6	2, 3, 4, 6, 7	
6	57.0, CH	2.31, br d (8.4)	5a, 5b	1, 2, 3, 4, 5, 7, 8, 20	1b, 8b, 10
7	21.6, C				
8	26.2, CH_2	a: 0.66, dd (8.4, 4.2)	8b, 9	6, 7, 9, 10, 20	20, 23
		b: 0.37, t (4.8)	8a, 9	6, 7, 9, 10, 20	6, 10, 16
9	28.9, CH	0.12, ddd (10.2, 8.4, 4.8)	8a, 8b, 10	6, 7, 8, 15, 20	15, 20, 21, 23
10	47.9, CH	1.32	9, 15	1, 8, 9, 11, 12, 14, 15, 21	1b, 6, 8b, 16, 22
11	44.6, C				
12	29.8, CH_2	a: 2.13, br d (13.8)	12b, 13a, 13b	10, 11, 13, 14, 21	1a
		b: 1.24	12a, 13a, 13b,	1, 10, 11, 13, 14, 21	1b
13	35.4, CH_2	a: 1.45	12a, 12b, 13b	11, 12, 14, 15, 18, 22	
		b: 1.30	12a, 12b, 13a	11, 12, 14, 15, 18, 22	21
14	42.8, C				
15	51.1, CH	1.19	10, 16	9, 10, 11, 13, 14, 16, 17, 18, 22, 23	9, 18b, 21, 25
16	45.5, CH	1.74, br t (10.2)	15, 17a, 17b, 23	10, 15, 17, 18, 23, 24, 25	8b, 10, 22, 24
17	22.2, CH_2	a: 1.62	16, 17b, 18a, 18b	15, 16, 18, 23	22
		b: 1.44	16, 17a, 18a, 18b	14, 15, 16, 18, 23	24
18	39.8, CH_2	a: 1.37	17a, 17b, 18b	13, 14, 15, 16, 17, 22	
		b: 1.00	17a, 17b, 18a	13, 14, 22	15
19	170.7, C				
20	20.7, CH_3	0.91, s		6, 7, 8, 9	4, 5a, 8a, 9, 21
21	61.2, CH_2	3.60, s		1, 10, 11, 12	9, 13b, 15, 20
22	17.7, CH_3	0.76, s		13, 14, 15, 18	10, 16, 17a
23	28.4, CH	2.23	16, 24, 25	15, 16, 17, 24, 25	8a, 9
24	23.1, CH_3	0.85, d (7.2)	23	16, 23, 25	16, 17b
25	15.0, CH_3	0.75, d (6.6)	23	16, 23, 24	15

[a] The indiscernible signals from overlap or the complex multiplicity are reported without designating multiplicity.

Table S4. NMR assignments for 3 (^{1}H for 600 MHz and ^{13}C for 150 MHz in $CDCl_3$)

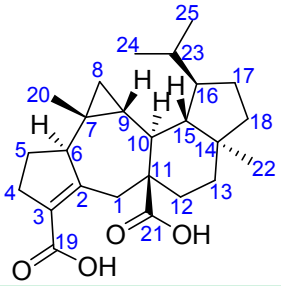

No.	δ_C, type	δ_H (J in Hz)[a]	^{1}H–^{1}H COSY	HMBC	ROESY
1	42.0, CH_2	a: 3.69, d (14.4)	1b	2, 3, 6, 10, 11, 12, 21	12a
		b: 2.10, d (14.4)	1a	2, 3, 11, 21	6, 10, 12b
2	156.9, C				
3	128.4, C				
4	32.9, CH_2	2.60	5	2, 3, 5	20
5	26.0, CH_2	1.95	4, 6	2, 3, 4, 6, 7	20
6	56.1, CH	2.40, br d (5.4)	5	2, 3, 4, 5, 7, 8, 20	1b, 8b, 10
7	21.8, C				
8	24.8, CH_2	a: 0.64	8b, 9	6, 7, 9, 10, 20	20, 23
		b: 0.40, br s	8a, 9	6, 7, 9, 10, 20	6, 10, 16
9	27.7, CH	0.67	8a, 8b, 10	6, 7, 8, 20	15, 20
10	46.4, CH	1.38	9, 15	1, 7, 8, 9, 11, 14, 15, 16, 21	1b, 6, 8b
11	51.8, C				
12	34.8, CH_2	a: 1.92	12b, 13	13	1a
		b: 1.63	12a, 13	1, 13, 14, 21	1b
13	35.8, CH_2	1.53	12a, 12b	11, 12, 15, 18	15
14	42.3, C				
15	50.0, CH	1.85, t (10.8)	10, 16	10, 11, 13, 14, 16, 22, 23	9, 13, 18b, 25
16	45.3, CH	1.74, br t (10.2)	15, 17a, 17b, 23	15, 17	8b, 22, 24
17	21.9, CH_2	a: 1.61	16, 17b, 18a, 18b	14, 16, 18, 23	22
		b: 1.46	16, 17a, 18a, 18b	14, 23	24, 25
18	39.7, CH_2	a: 1.39	17a, 17b, 18b	14, 15, 16, 22	
		b: 1.07	17a, 17b, 18a	13, 14, 17, 22	15
19	170.8, C				
20	20.3, CH_3	0.86, s		6, 7, 8, 9	4, 5, 8a, 9
21	182.0, C				
22	17.7, CH_3	0.73, s		13, 14, 15, 18	16, 17a
23	28.4, CH	2.32	16, 24, 25	16, 17, 24, 25	8a
24	23.1, CH_3	0.86, d (6.6)	23	16, 23, 25	16, 17b
25	15.2, CH_3	0.79, d (6.6)	23	16, 23, 24	15, 17b

[a] The indiscernible signals from overlap or the complex multiplicity are reported without designating multiplicity.

.

Table S5. NMR assignments for 4 (^{1}H for 600 MHz and ^{13}C for 150 MHz in $CDCl_3$)

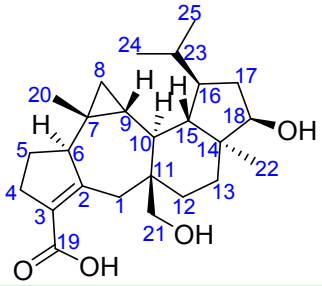

No.	δ_C, type	δ_H (J in Hz)[a]	^{1}H–^{1}H COSY	HMBC	ROESY
1	42.9, CH_2	a: 3.47, d (13.8)	1b	2, 3, 6, 10, 11, 12	12a
		b: 1.58, d (13.8)	1a	2, 3, 6, 10, 11, 21	6, 10, 12b
2	159.5, C				
3	127.8, C				
4	32.9, CH_2	2.60	5	2, 3	20
5	26.1, CH_2	2.00	4, 6	2, 3, 4, 6, 7	20
6	57.0, CH	2.29, br d (8.4)	5	1, 2, 3, 4, 5, 7, 8, 20	1b, 8b, 10
7	21.8, C				
8	26.6, CH_2	a: 0.68, dd (7.8, 4.2)	8b, 9	6, 7, 9, 10, 20	23
		b: 0.39, t (4.2)	8a, 9	6, 7, 9, 10, 20	6, 10, 16
9	28.9, CH	0.15	8a, 8b, 10	6, 8, 15, 20	15, 20, 21a, 21b, 23
10	47.8, CH	1.40, t (10.8)	9, 15	1, 8, 9, 11, 12, 14, 15, 16, 21	1b, 6, 8b, 16, 22
11	44.6, C				
12	29.3, CH_2	a: 2.17, br dd (13.2, 3.6)	12b, 13a, 13b	10, 11, 13, 14, 21	1a
		b: 1.20	12a, 13a, 13b	10, 11, 13, 14, 21	1b
13	28.1, CH_2	a: 1.73	12a, 12b, 13b	11, 12, 14, 15, 18, 22	21a
		b: 1.20	12a, 12b, 13a	11, 12, 14, 15, 22	18
14	47.4, C				
15	45.7, CH	1.64, t (10.8)	10, 16	9, 10, 16, 22, 23	9, 21a, 21b, 25
16	45.7, CH	1.77	15, 17a, 17b, 23	17, 23, 24, 25	8b, 10, 22, 24
17	32.1, CH_2	a: 2.04	16, 17b, 18	15, 16, 23	22
		b: 1.36, br dd (15.0, 4.8)	16, 17a, 18	14, 15, 16, 18, 23	24, 25
18	78.0, CH	3.66, br d (6.0)	17a, 17b	15, 16, 22	13b, 22
19	170.1, C				
20	20.7, CH_3	0.91, s		6, 7, 8, 9	4, 5, 9, 21b
21	60.9, CH_2	a: 3.68, d (12.0)	21b	1, 11, 12	9, 13a, 15
		b: 3.59, d (12.0)	21a	1, 11, 12	9, 15, 20
22	17.7, CH_3	0.72, s		13, 14, 15, 18	10, 16, 17a, 18
23	27.6, CH	2.32	16, 24, 25	15, 16, 17, 24, 25	8a, 9
24	23.1, CH_3	0.82, d (6.6)	23	16, 23, 25	16, 17b
25	15.6, CH_3	0.80, d (6.6)	23	16, 23, 24	15, 17b

[a] The indiscernible signals from overlap or the complex multiplicity are reported without designating multiplicity.

Table S6. The Boltzmann distribution for two possible structures (A and B) of 4

A		B	
Conformers	Contribution (%)	Conformers	Contribution (%)
1	23.44	1	23.31
2	23.38	2	19.11
3	9.86	3	11.51
4	8.69	4	8.63
5	7.87	5	7.75
6	7.50	6	7.49
7	6.04	7	7.49
8	5.52	8	6.06
9	3.26	9	4.94
10	3.06	10	1.33
11	1.37	11	1.33
		12	1.05

Supplementary Figures

A

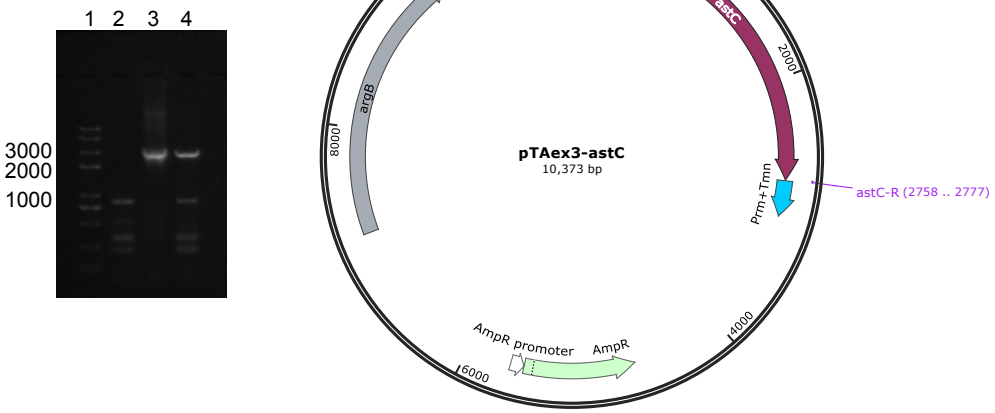

1 Marker
2 *astC* amplified from *A. oryzae* host strain
3 *astC* amplified from pTAex3-*astC*
4 *astC* amplified from transformant harboring pTAex3-*astC*

B

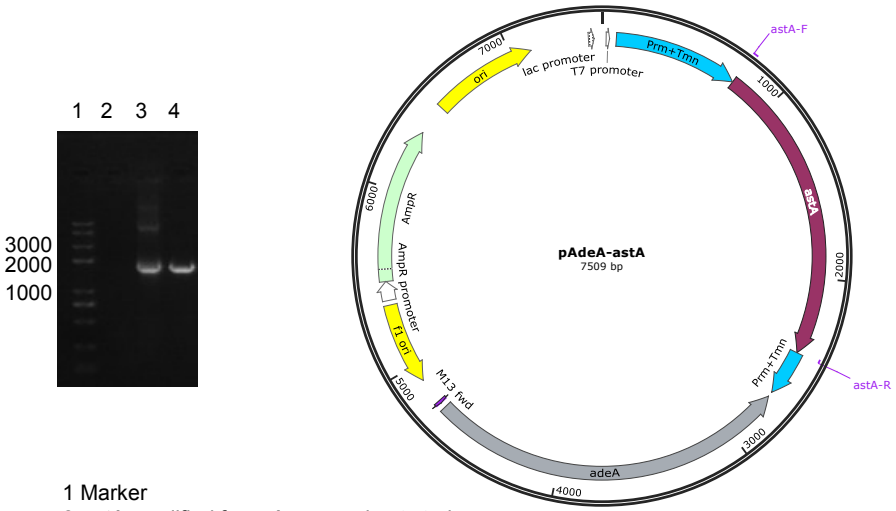

1 Marker
2 *astA* amplified from *A. oryzae* host strain
3 *astA* amplified from pAdeA-*astA*
4 *astA* amplified from transformant harboring pTAex3-*astC* and pAdeA-*astA*

C

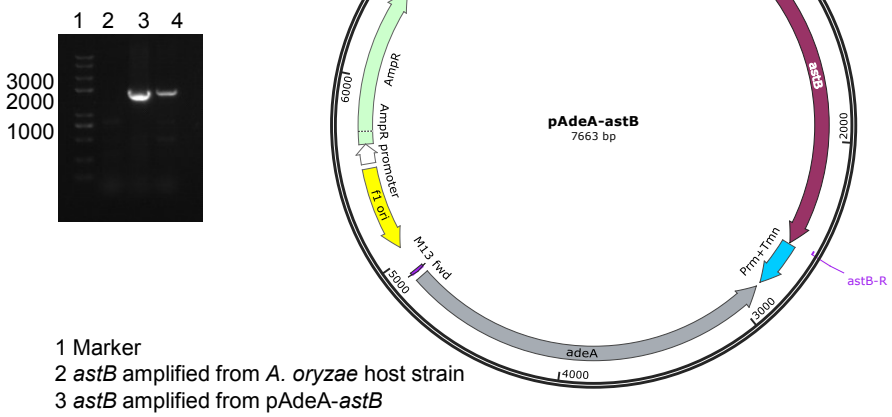

1 Marker
2 *astB* amplified from *A. oryzae* host strain
3 *astB* amplified from pAdeA-*astB*
4 *astB* amplified from transformant harboring pTAex3-*astC* and pAdeA-*astB*

D

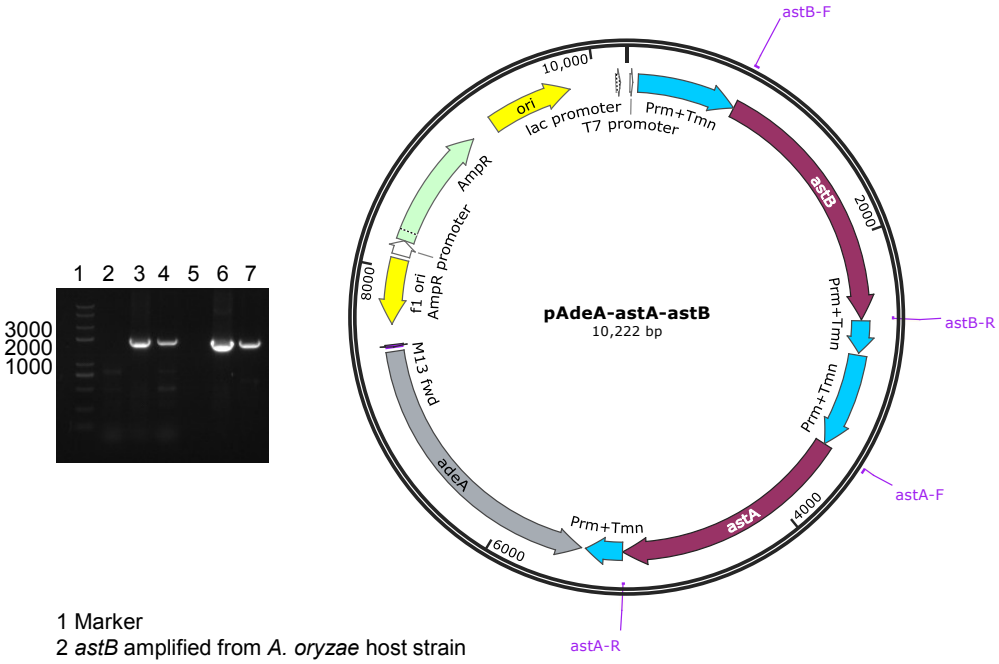

1 Marker
2 *astB* amplified from *A. oryzae* host strain
3 *astB* amplified from pAdeA-*astA*-*astB*
4 *astB* amplified from transformant harboring pTAex3-*astC* and pAdeA-*astA*-*astB*
5 *astA* amplified from *A. oryzae* host strain
6 *astA* amplified from pAdeA-*astA*-*astB*
7 *astA* amplified from transformant harboring pTAex3-*astC* and pAdeA-*astA*-*astB*

Fig. S1. PCR analysis for confirmation of the transformants

(A) PCR verification of introduction of pTAex3-*astC* into the *A. oryzae* host strain (left) and the pTAex3-*astC* map (right); (B) PCR verification of introduction of pAdeA-*astA* into the transformant harboring pTAex3-*astC* (left) and the pAdeA-*astA* map (right); (C) PCR verification of introduction of pAdeA-*astB* into the transformant harboring pTAex3-*astC* (left)

and the pAdeA-*astB* map (right); (D) PCR verification of introduction of pAdeA-*astA*-*astB* into the transformant harboring pTAex3-*astC* (left) and the pAdeA-*astA*-*astB* map (right).

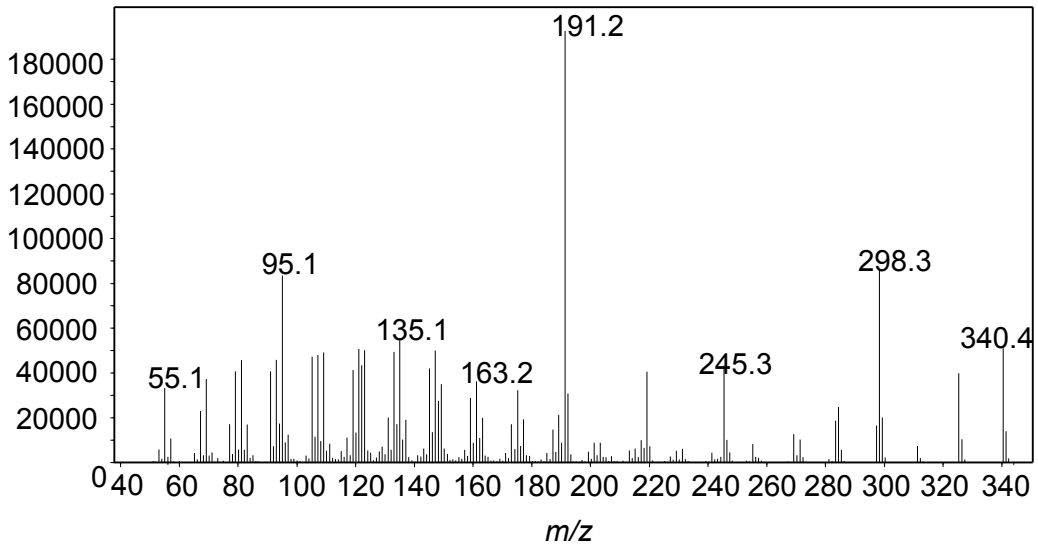

Fig. S2. Electron impact mass spectrum of 1

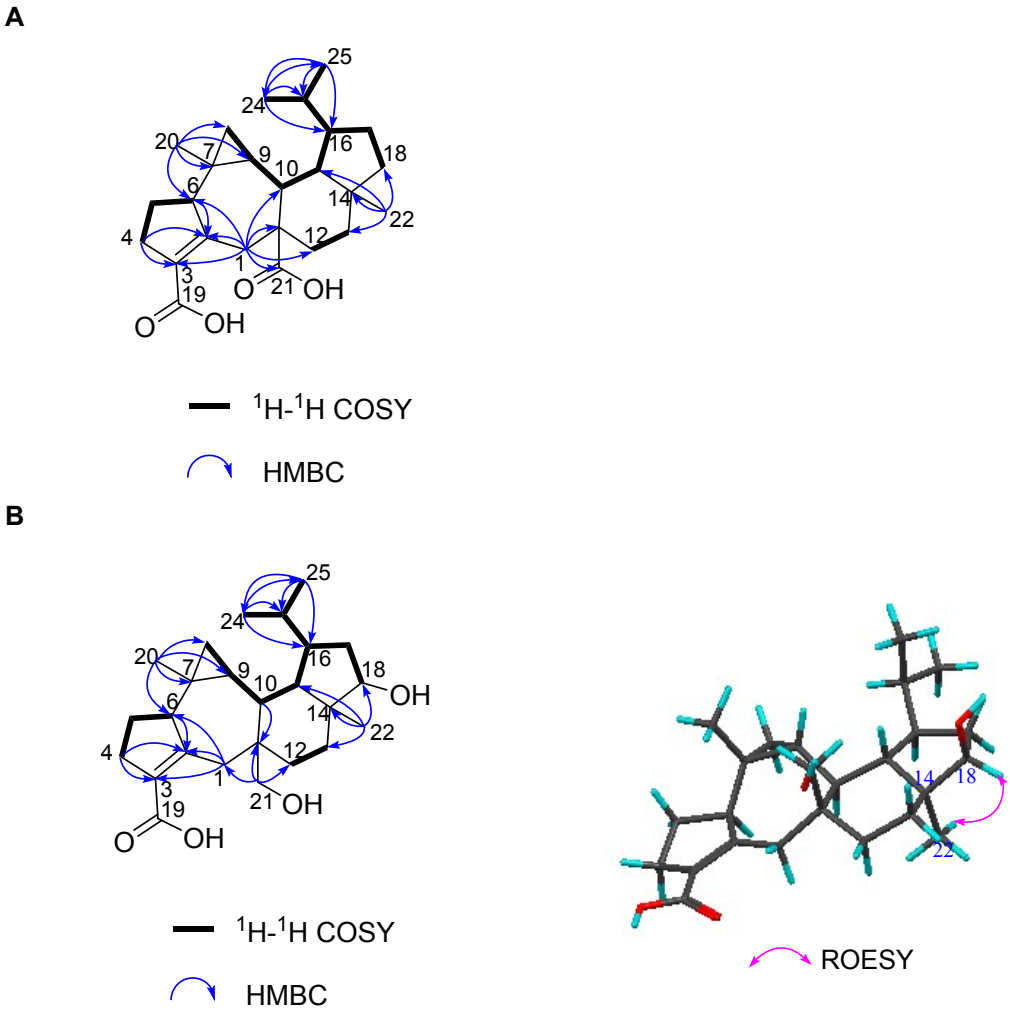

Fig. S3. Key ^{1}H-^{1}H COSY, HMBC and ROESY correlations for 3 (A) and 4 (B)

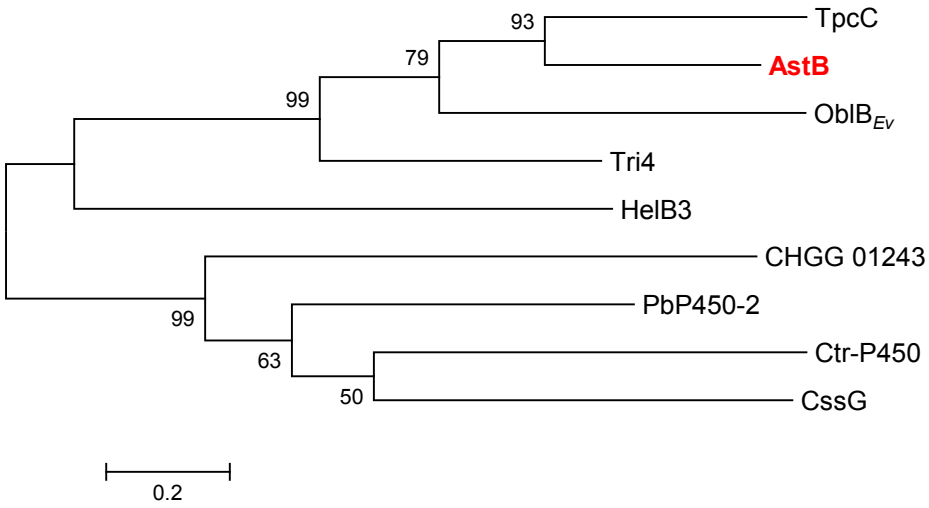

Fig. S4. Phylogenetic analysis of the multifunctional P450s in fungi

The phylogenetic tree was constructed using MEGA 6.0. The sequence data of these proteins can be retrieved according to the Genbank accession TpcC (EMD93706.1),[8] OblB$_{Ev}$ (BAX09283.1),[9] Tri4 (BAF36546.1),[10] HelB3 (XP_751352.2),[11] CHGG 01243 (XP_001220464.1),[12] PbP450-2 (Q6F5E2.1),[13] Ctr-P450 (BAW27598.1),[14] and CssG (XP_001270548.1).[15]

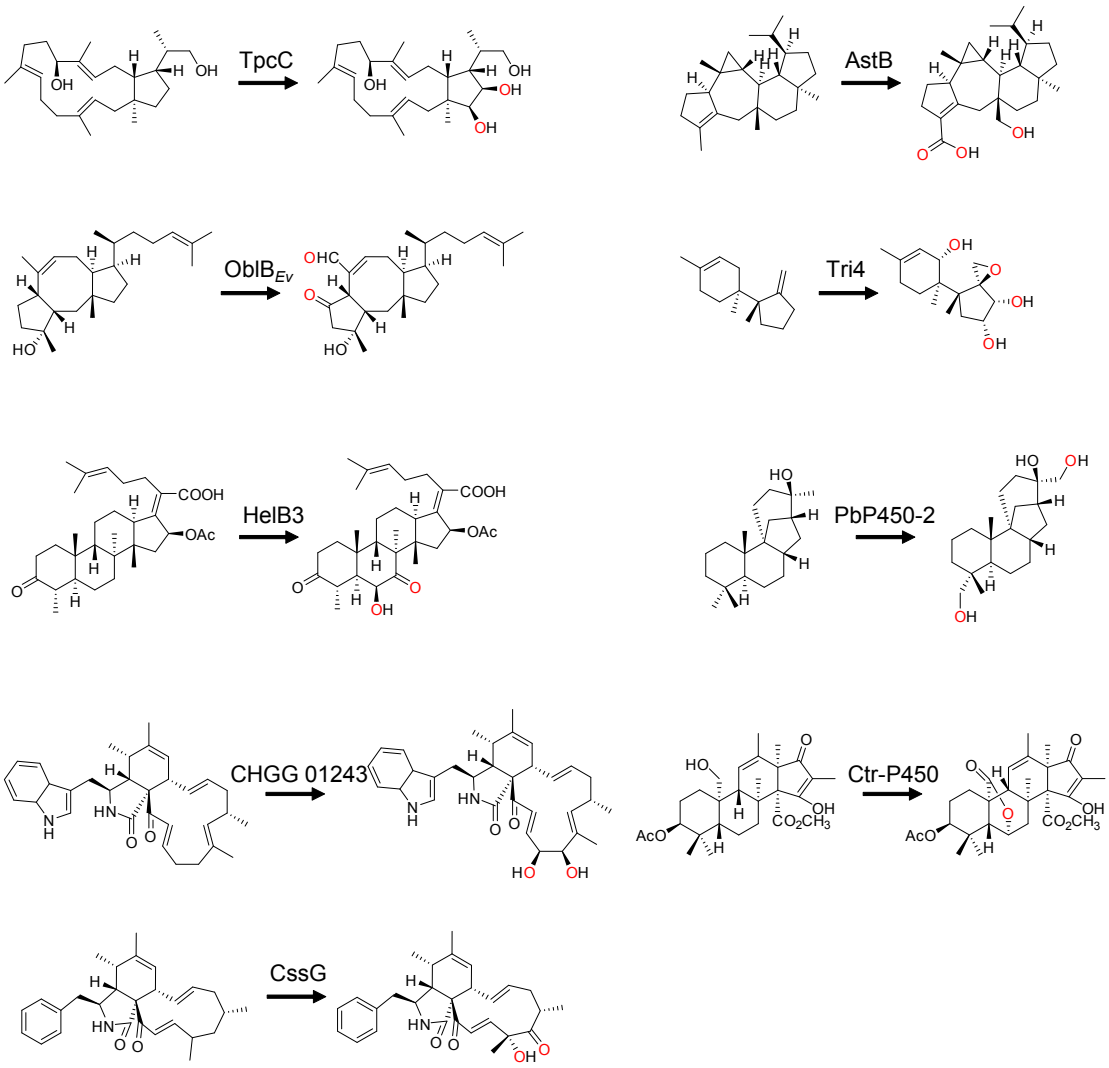

Fig. S5. Representatives of multiple oxidation reactions catalyzed by P450s in fungi

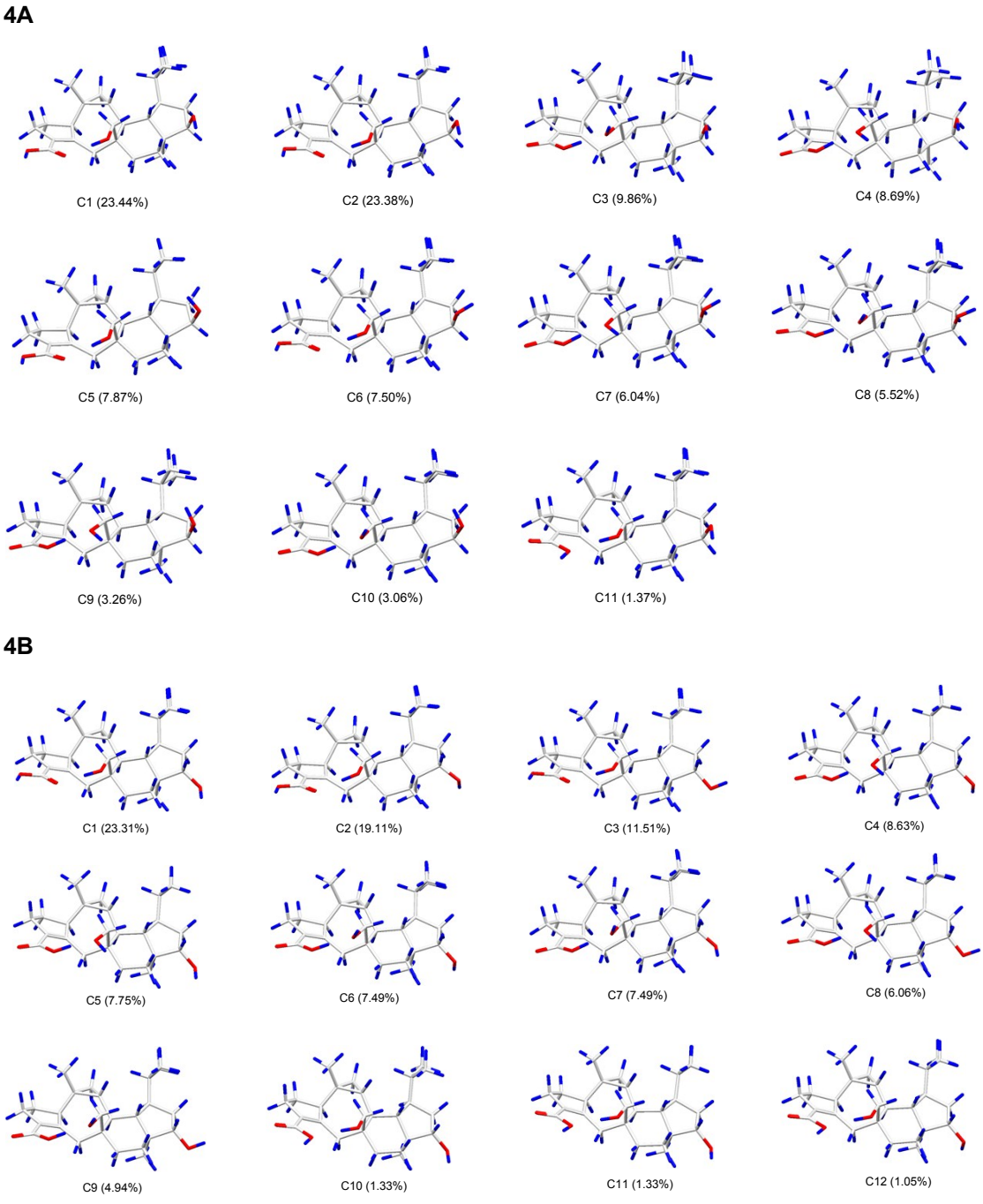

Fig. S6. Most stable conformers of 4A and 4B

(6*S**, 7*R**, 9*R**, 10*S**, 11*S**, 14*S**, 15*S**, 16*R**, 18*R**)–**4A** and (6*S**, 7*R**, 9*R**, 10*S**, 11*S**, 14*S**, 15*S**, 16*R**, 18*S**)–**4B** (the relative populations are in parentheses)

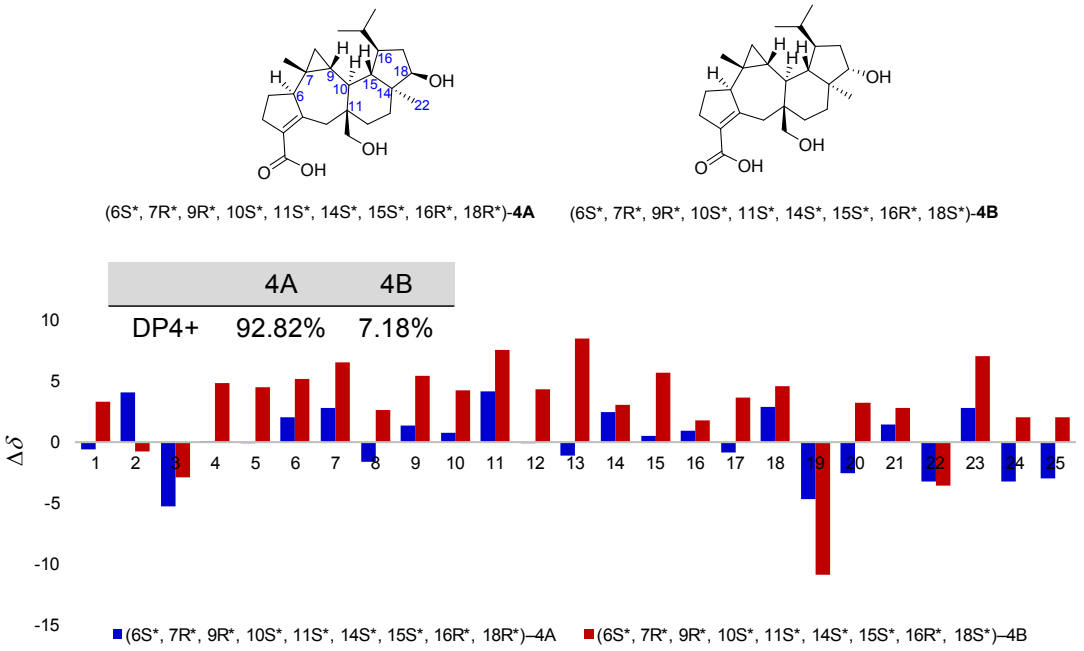

Fig. S7. Differences between NMR chemical shifts of 4 and theoretical ^{13}C NMR chemical shifts for 4A and 4B

DP4+ denotes the probability analysis of **4A** and **4B**.

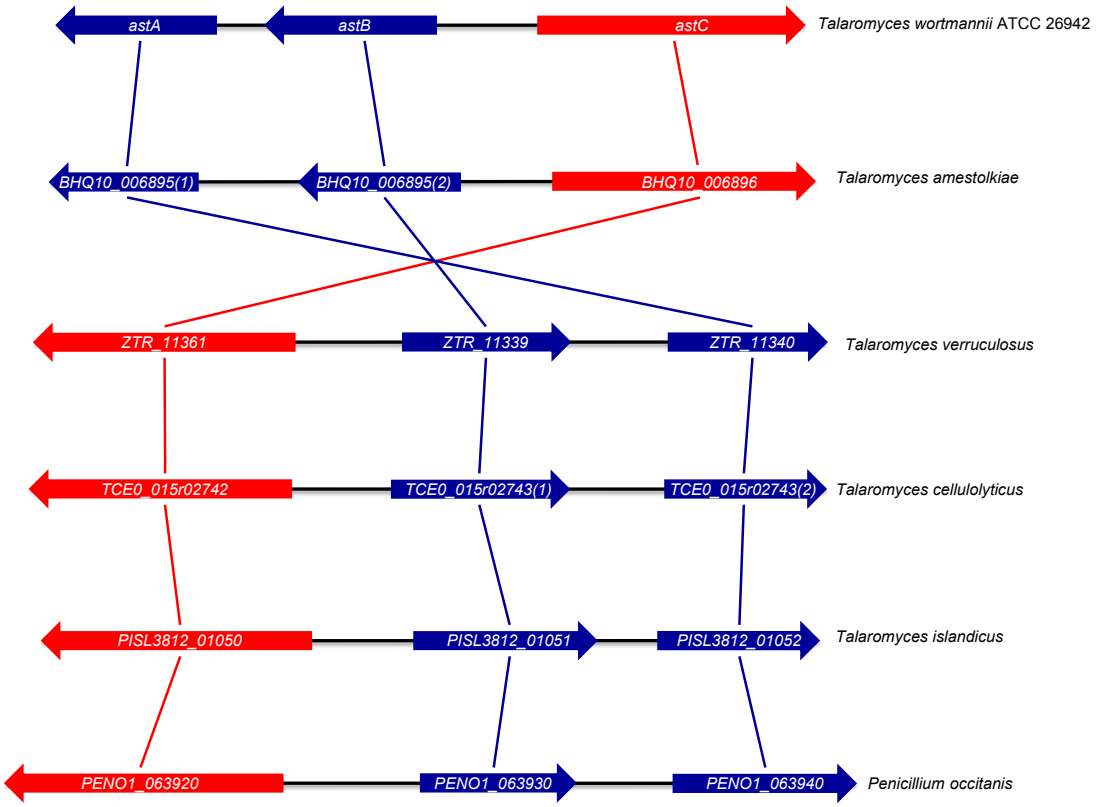

Fig. S8. Homologues of the *astABC* cassette discovered in NCBI database.

The amino acid sequence similarities between AstA and its homologues, AstB and its homologues, and AstC and its homologues are all above 70%. BHQ10_006895(1) and BHQ10_006895(2), and TCE0_015r02743(1) and TCE0_015r02743(2) are manually revised in this work.

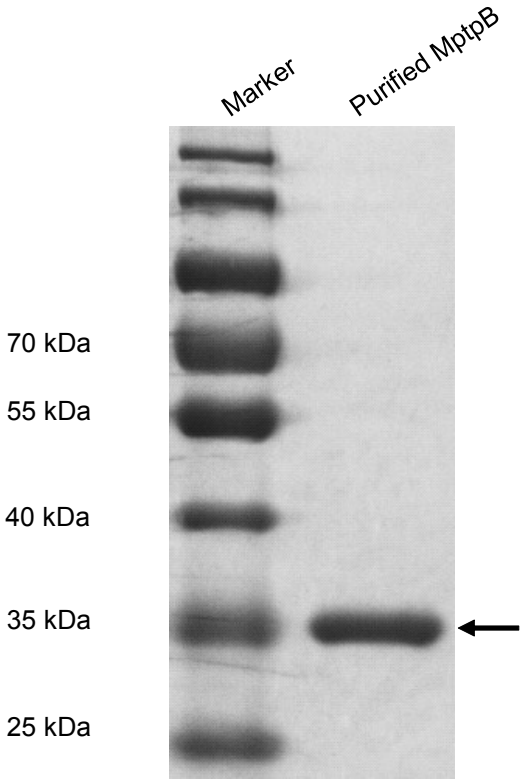

Fig. S9. SDS-PAGE analysis of purified recombinant MptpB

A

Compound	MptpB inhibition (%)
1	14.9
2	96.6
3	96.5
4	36.0
Sodium orthovanadate	94.9

B

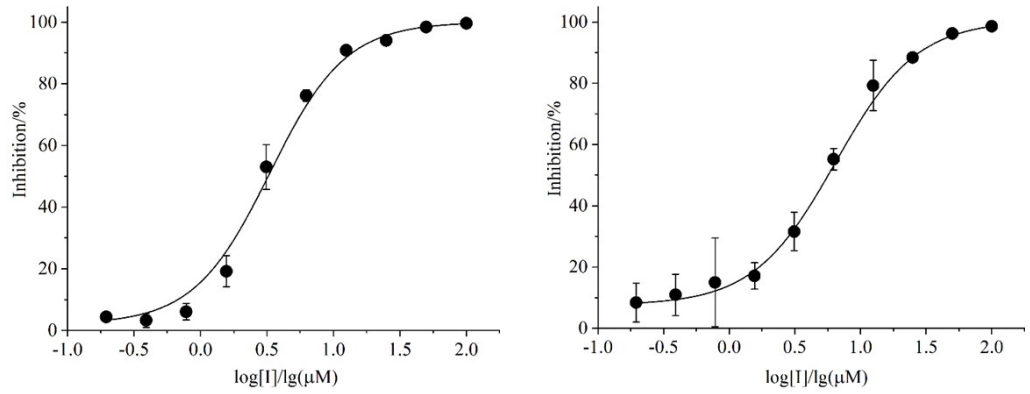

C

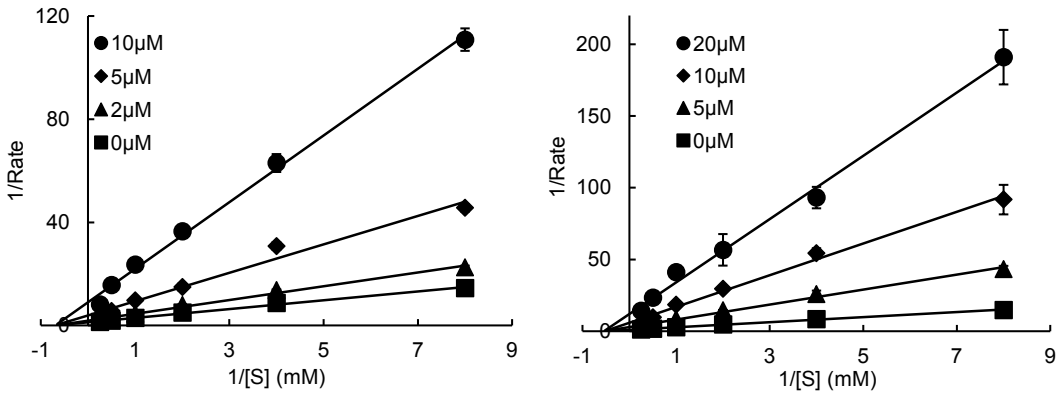

Fig. S10. Evaluation of the inhibitory activity against MptpB

(A) Percentage of inhibition at the concentration of 50 μM; (B) IC_{50} curves of **2** (left) and **3** (right); (C) Lineweaver-Burk plots for **2** (left) and **3** (right).

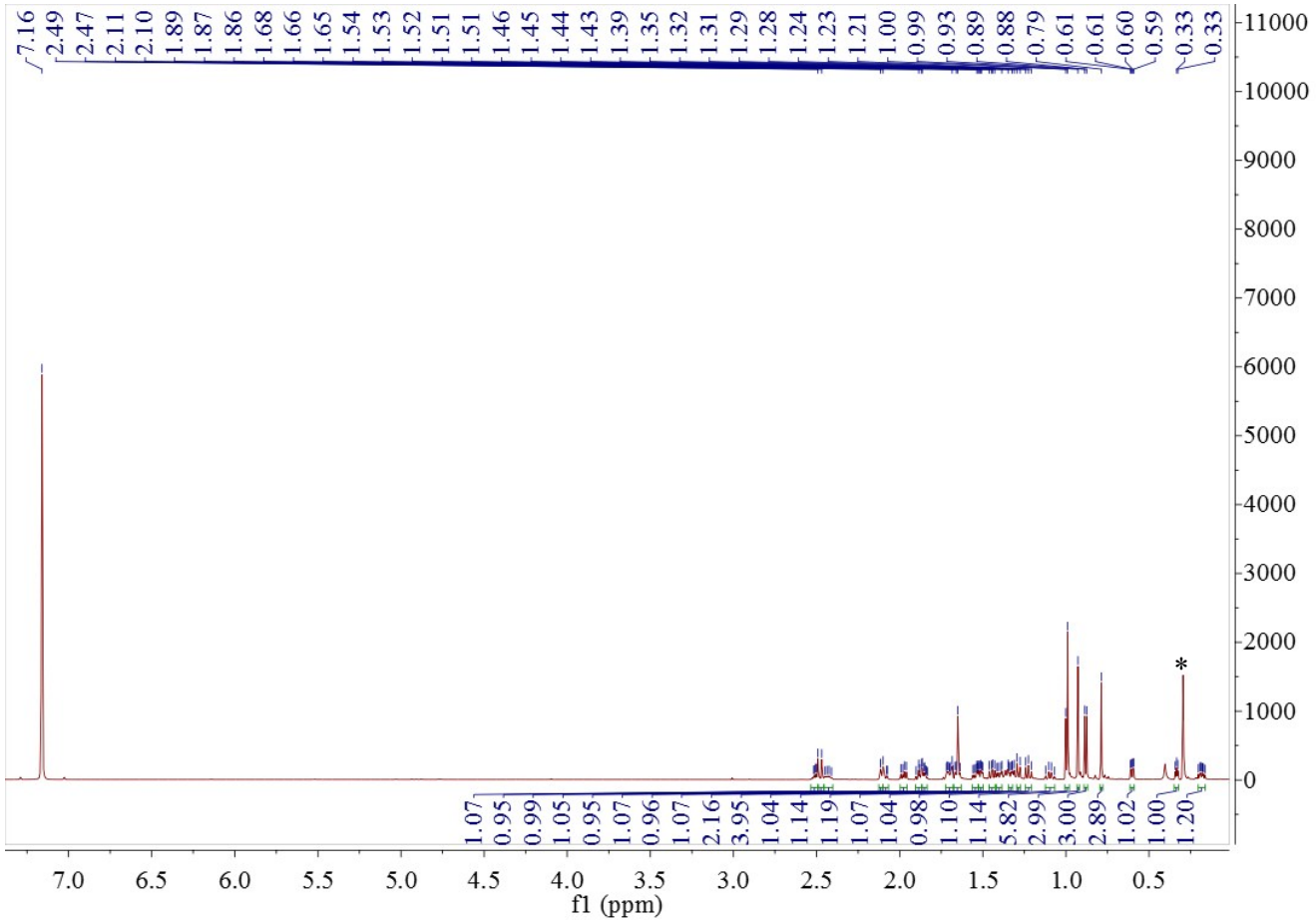

Fig. S11. ^{1}H NMR spectrum of 1 in C_6D_6 at 600 MHz

Asterisk indicates that the signal is from silicone grease.

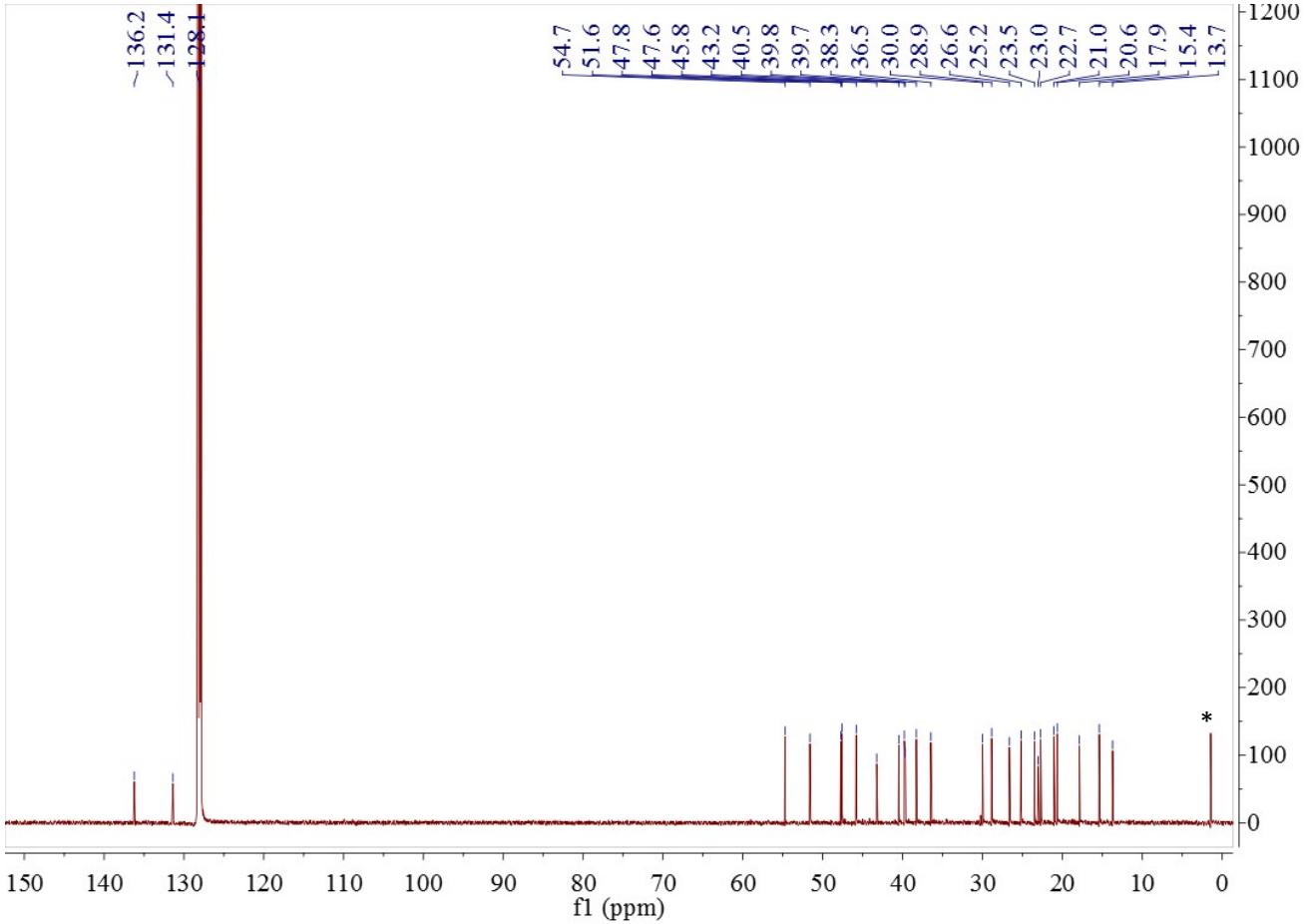

Fig. S12. ^{13}C NMR spectrum of 1 in C_6D_6 at 150 MHz

Asterisk indicates that the signal is from silicone grease.

Single Mass Analysis
Tolerance = 10.0 PPM / DBE: min = -1.5, max = 50.0
Element prediction: Off
Number of isotope peaks used for i-FIT = 3

Monoisotopic Mass, Even Electron Ions
86 formula(e) evaluated with 1 results within limits (all results (up to 1000) for each mass)
Elements Used:
C: 0-60 H: 0-100 O: 0-200
5150-4
2018091051 342 (2.749) Cm (336:342)

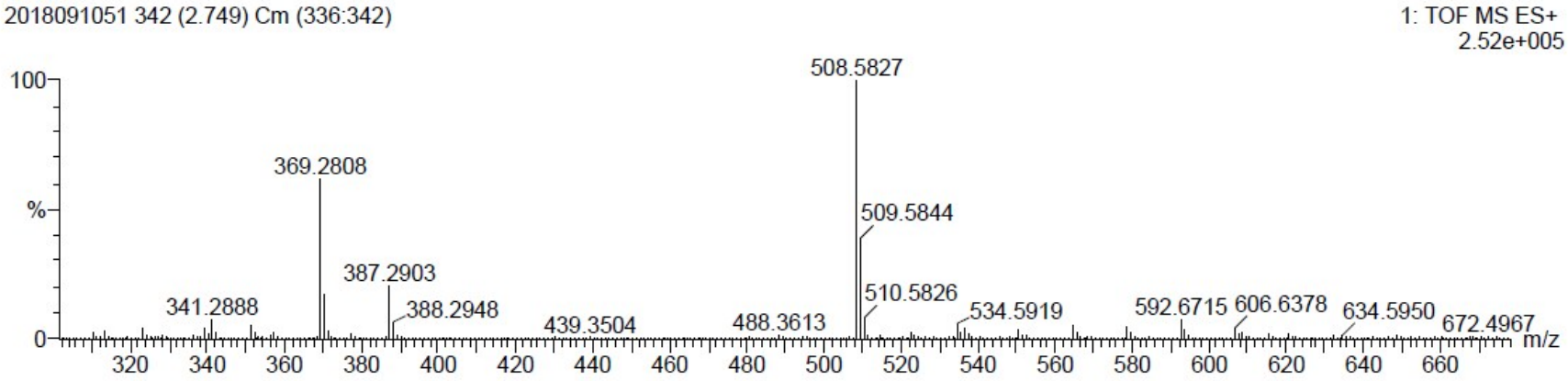

Minimum:				-1.5				
Maximum:		5.0	10.0	50.0				
Mass	Calc. Mass	mDa	PPM	DBE	i-FIT	Norm	Conf(%)	Formula
387.2903	387.2899	0.4	1.0	6.5	19.0	n/a	n/a	C25 H39 O3

Fig. S13. HRESIMS spectrum of 2

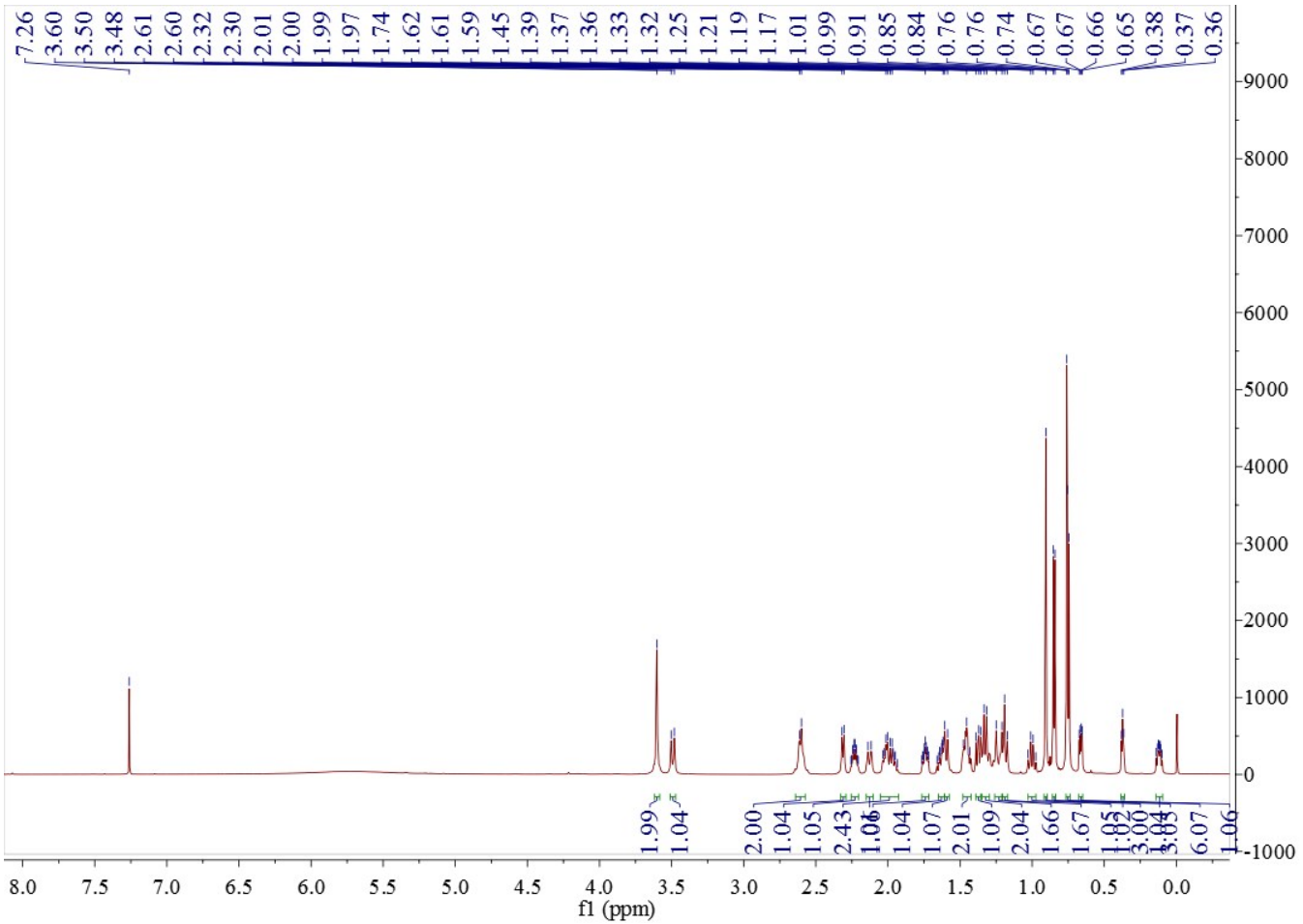

Fig. S14. ^{1}H NMR spectrum of 2 in $CDCl_3$ at 600 MHz

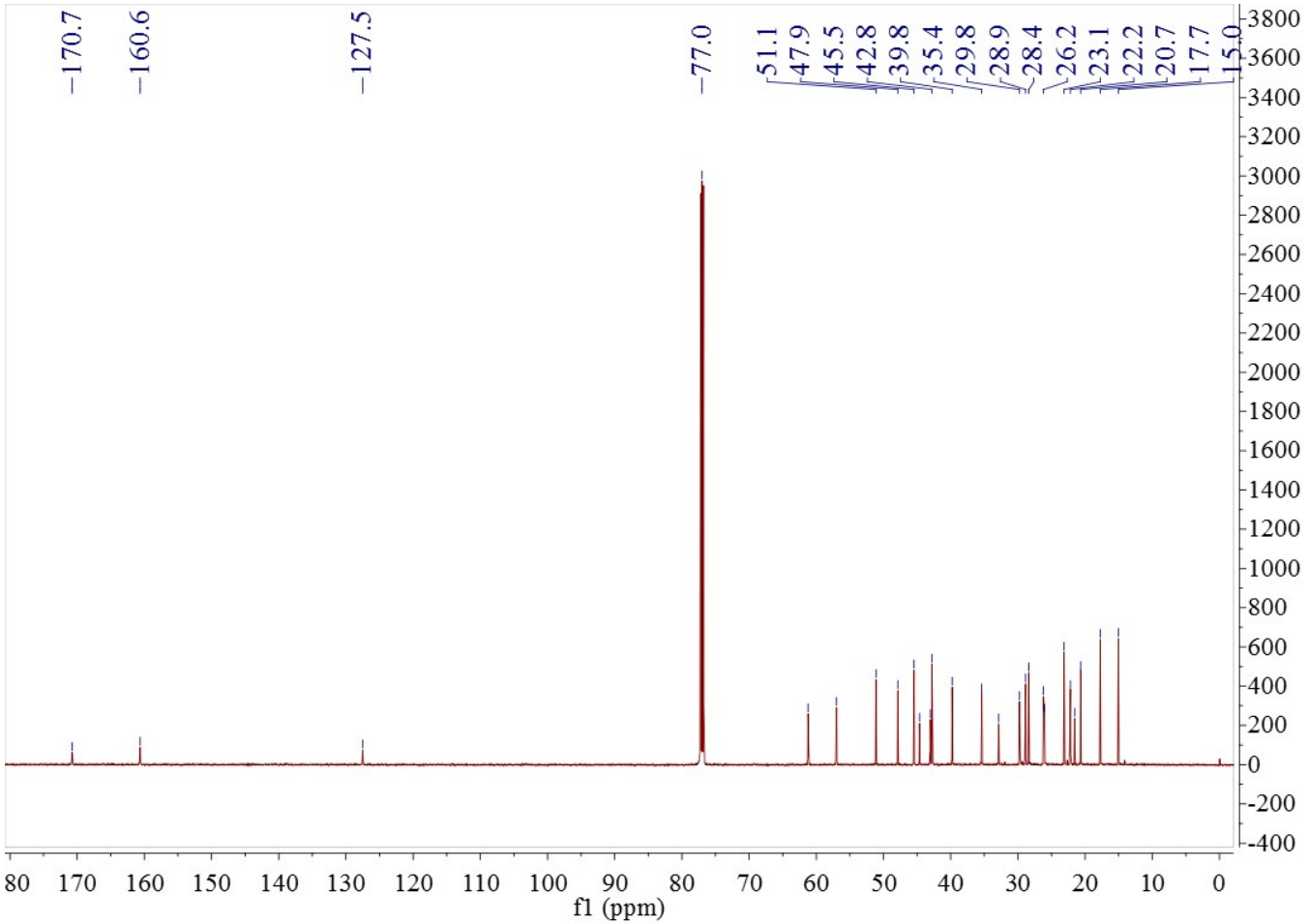

Fig. S15. ^{13}C NMR spectrum of 2 in $CDCl_3$ at 150 MHz

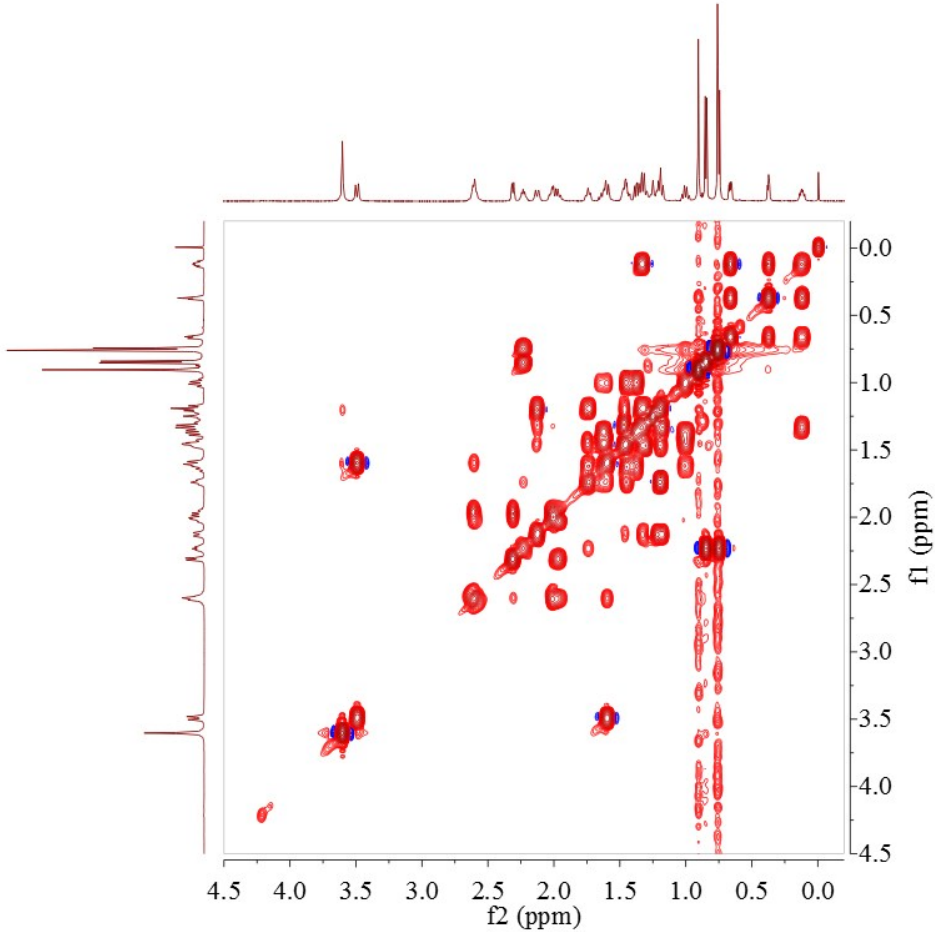

Fig. S16. ^{1}H-^{1}H COSY spectrum of 2 in $CDCl_3$ at 600 MHz

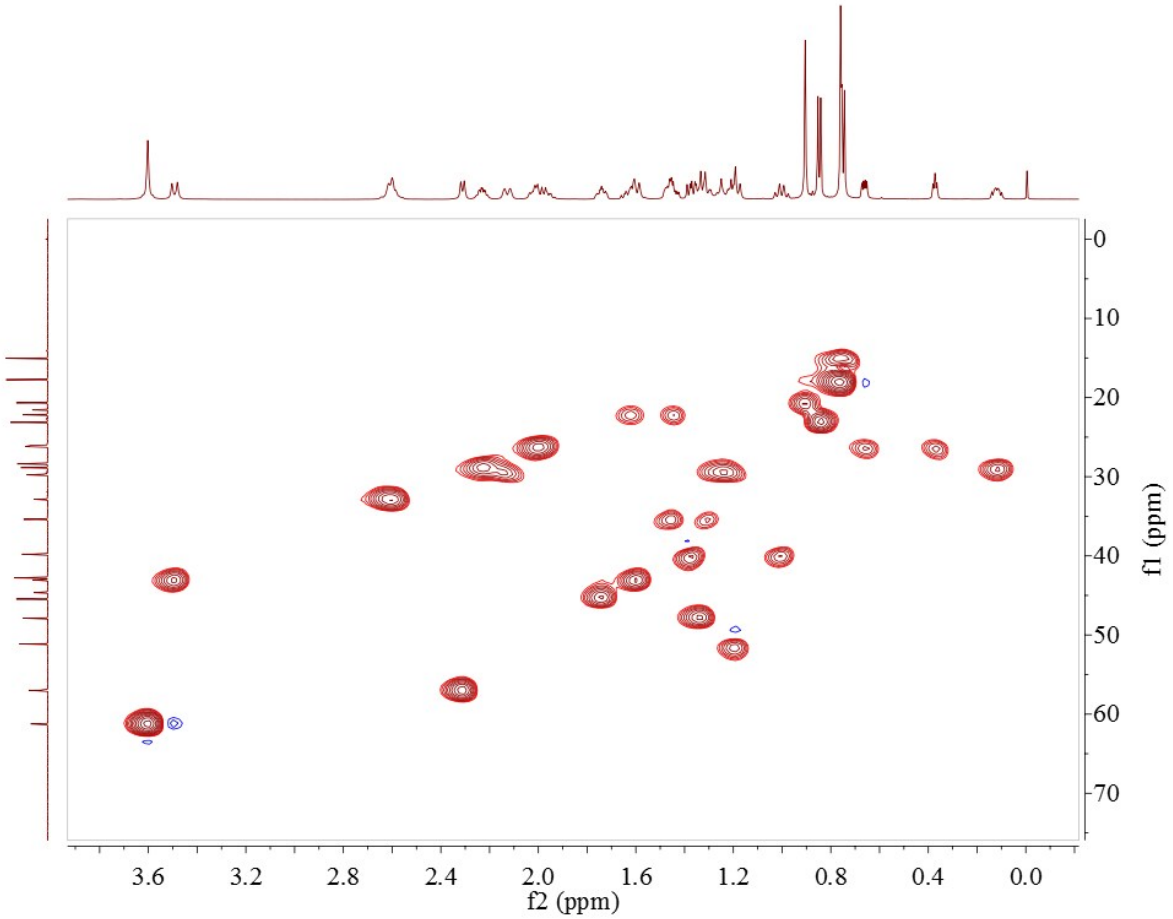

Fig. S17. HSQC spectrum of 2 in $CDCl_3$ at 600 MHz

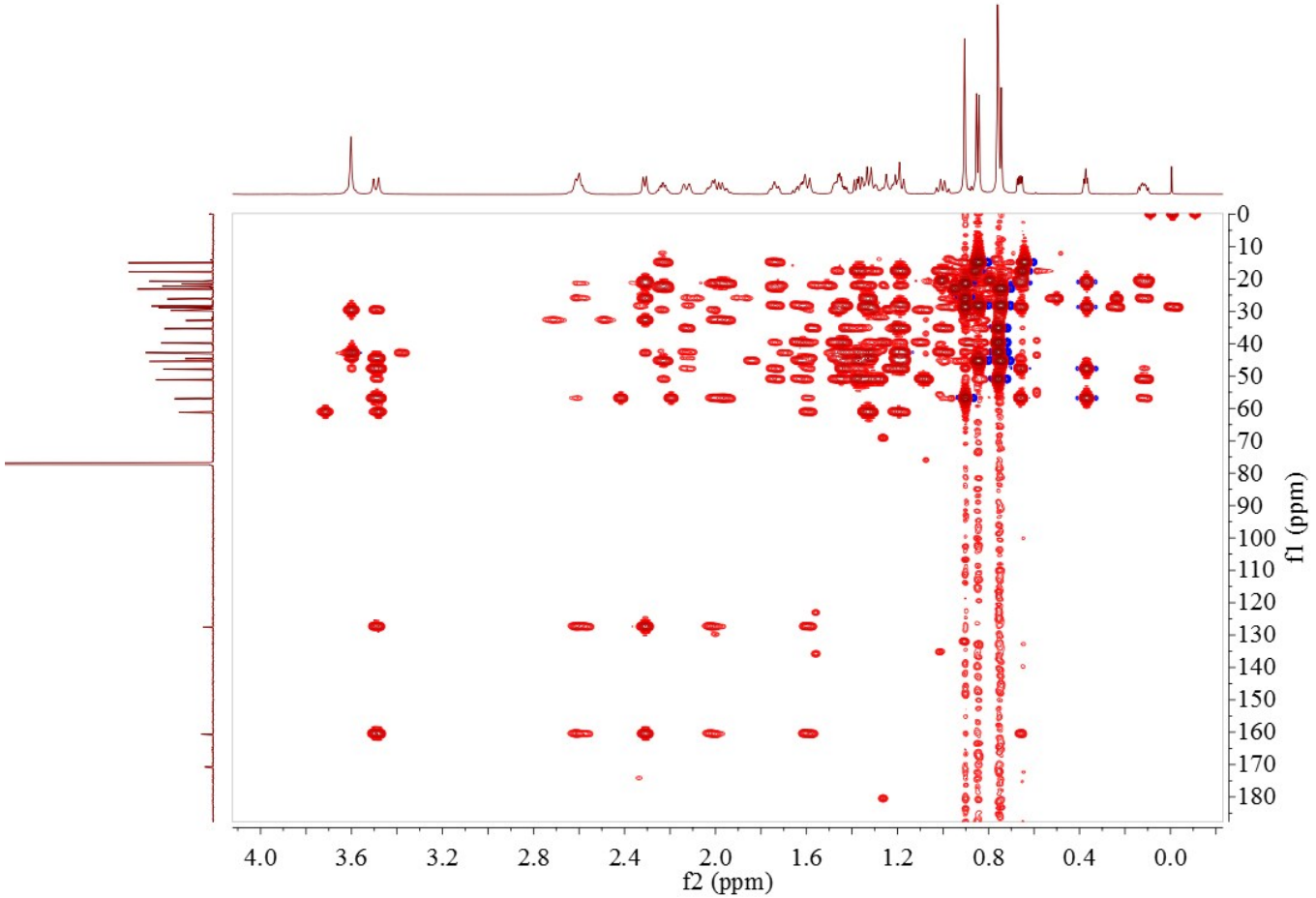

Fig. S18. HMBC spectrum of 2 in $CDCl_3$ at 600 MHz

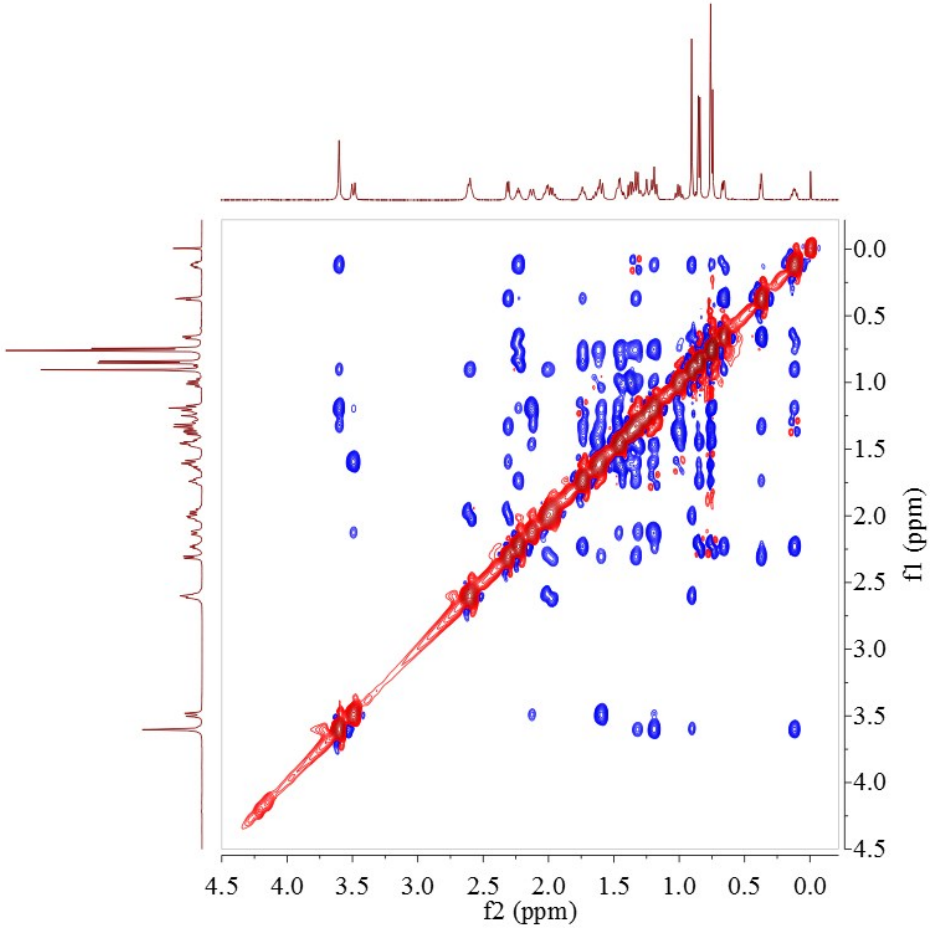

Fig. S19. ROESY spectrum of 2 in $CDCl_3$ at 600 MHz

Single Mass Analysis
Tolerance = 10.0 PPM / DBE: min = -1.5, max = 50.0
Element prediction: Off
Number of isotope peaks used for i-FIT = 3

Monoisotopic Mass, Even Electron Ions
260 formula(e) evaluated with 3 results within limits (all results (up to 1000) for each mass)
Elements Used:
C: 0-60 H: 0-100 O: 0-200
5150-3
2018091052 289 (2.330) Cm (287:299)

1: TOF MS ES+
5.08e+006

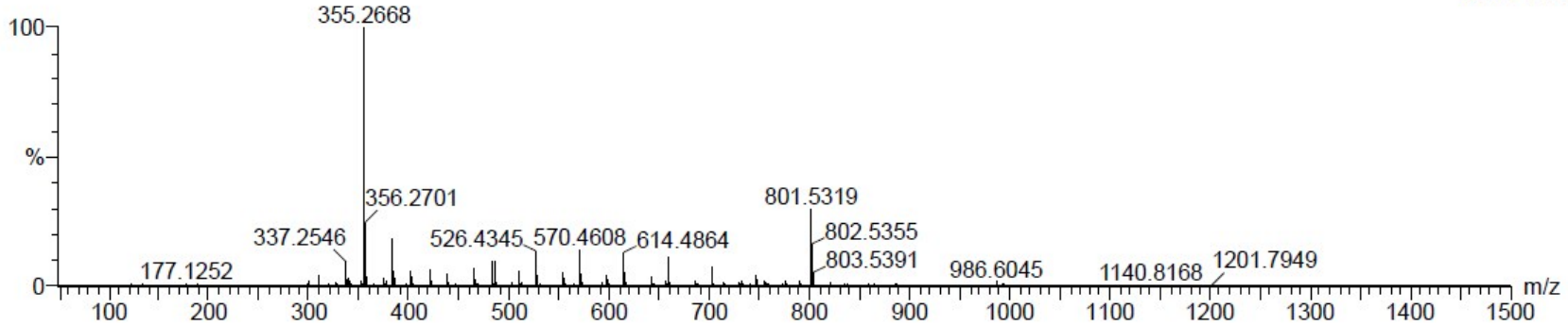

Minimum:				-1.5				
Maximum:		5.0	10.0	50.0				
Mass	Calc. Mass	mDa	PPM	DBE	i-FIT	Norm	Conf(%)	Formula
801.5319	801.5305	1.4	1.7	14.5	38.2	0.000	99.99	C50 H73 O8
	801.5364	-4.5	-5.6	5.5	47.5	9.287	0.01	C43 H77 O13
	801.5247	7.2	9.0	23.5	49.0	10.783	0.00	C57 H69 O3

Fig. S20. HRESIMS spectrum of 3

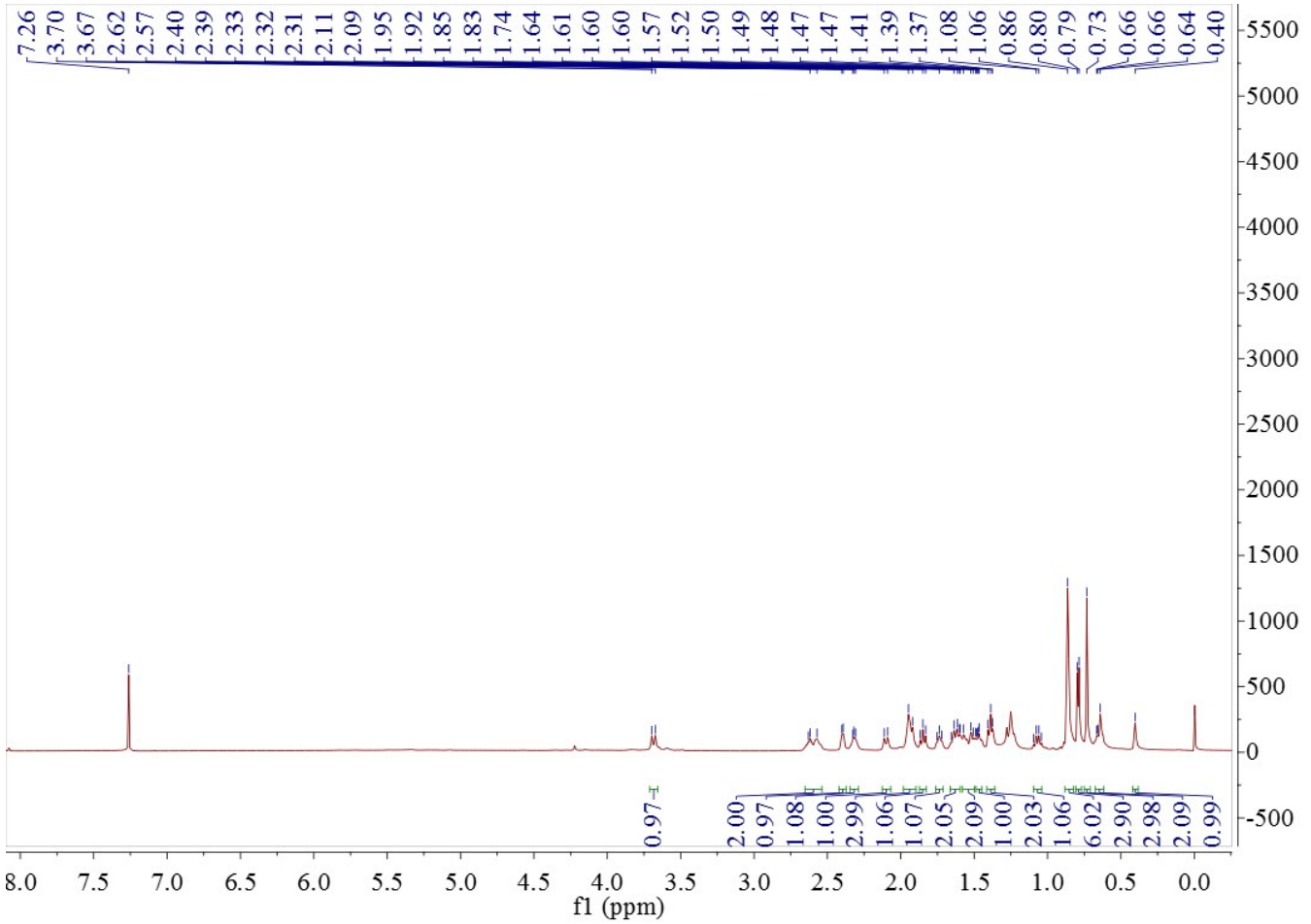

Fig. S21. ^{1}H NMR spectrum of 3 in $CDCl_3$ at 600 MHz

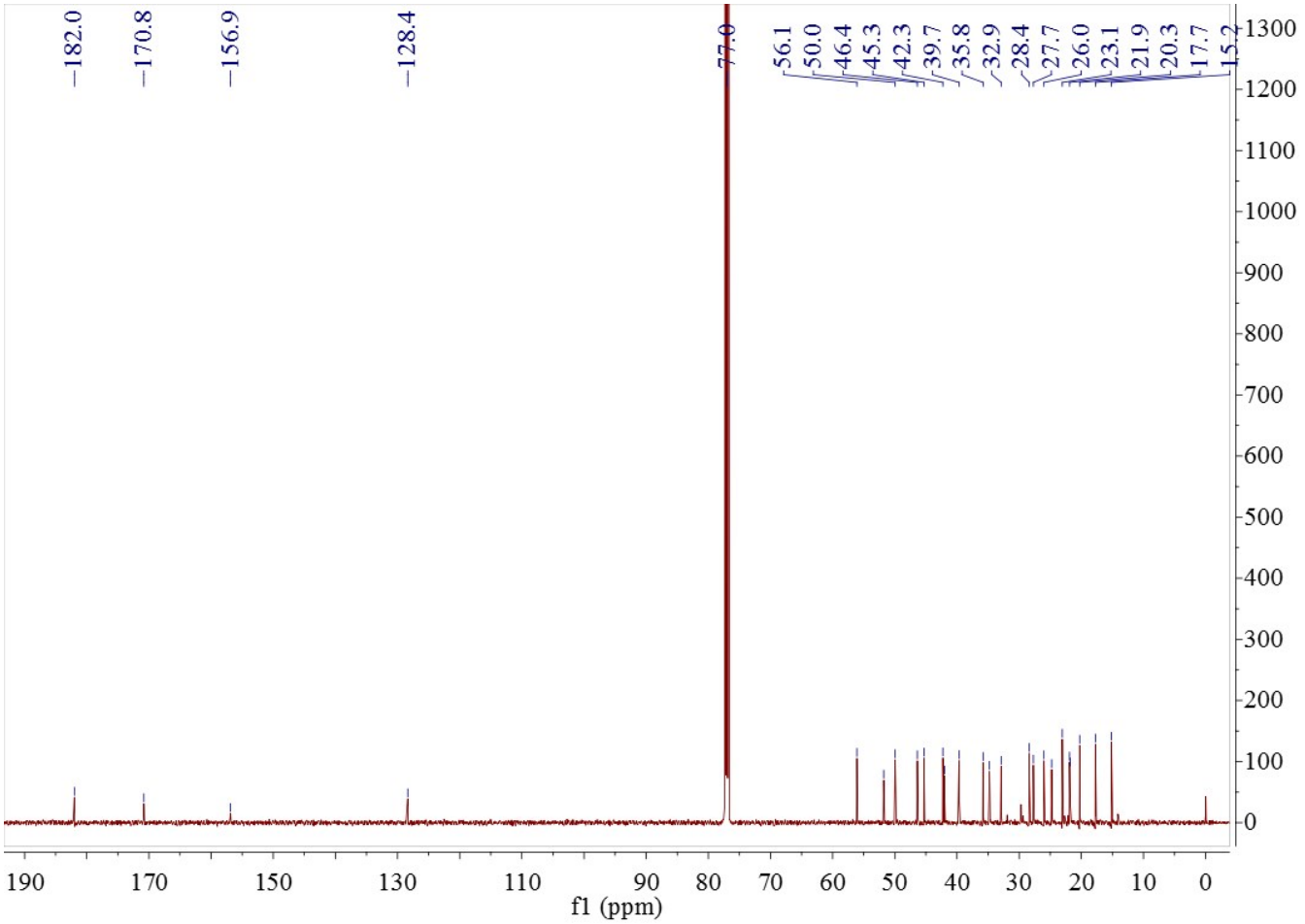

Fig. S22. ^{13}C NMR spectrum of 3 in $CDCl_3$ at 150 MHz

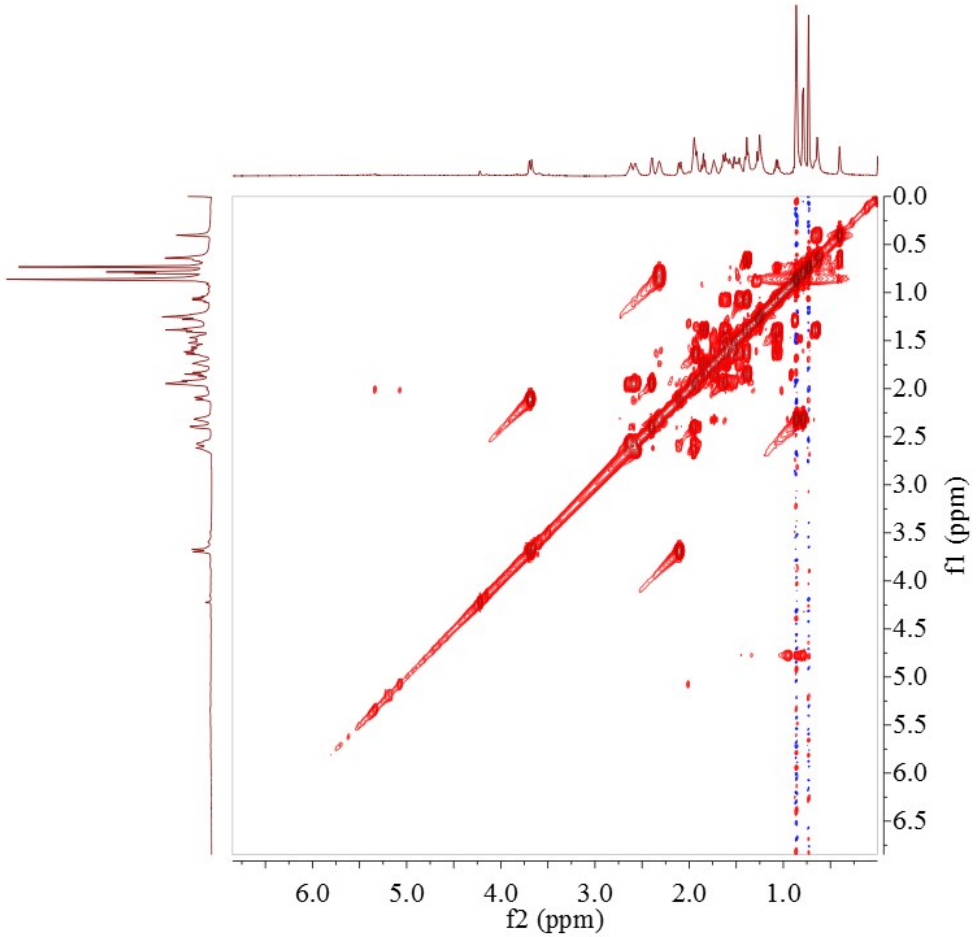

Fig. S23. ^{1}H-^{1}H COSY spectrum of 3 in $CDCl_3$ at 600 MHz

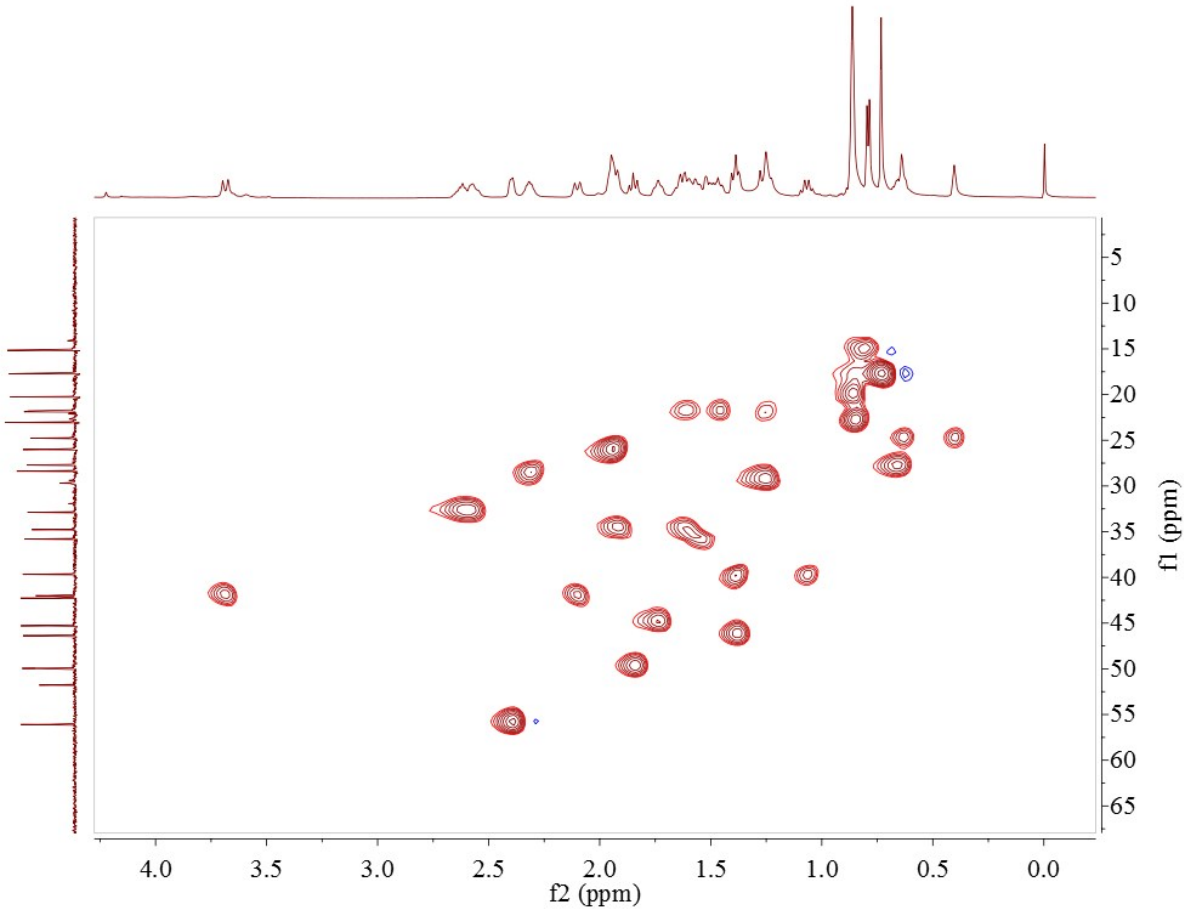

Fig. S24. HSQC spectrum of 3 in $CDCl_3$ at 600 MHz

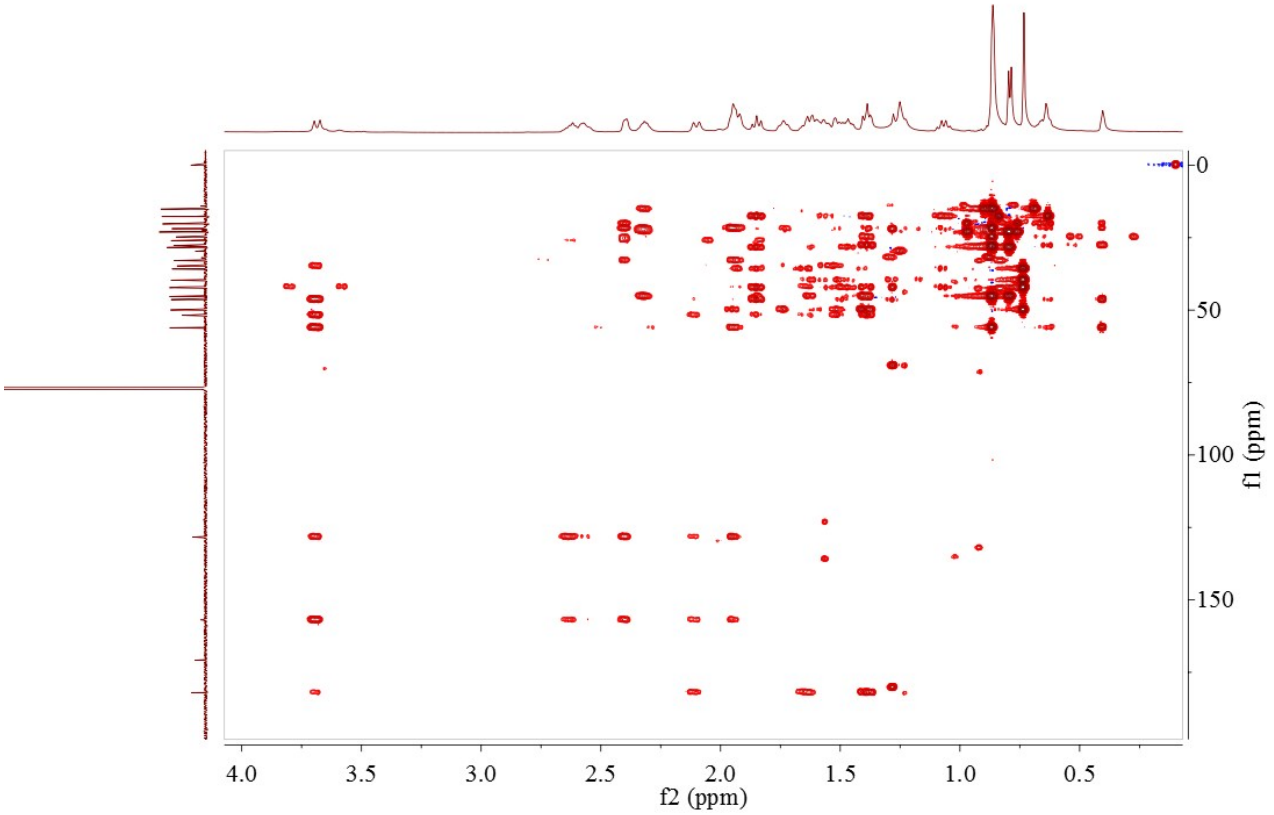

Fig. S25. HMBC spectrum of 3 in $CDCl_3$ at 600 MHz

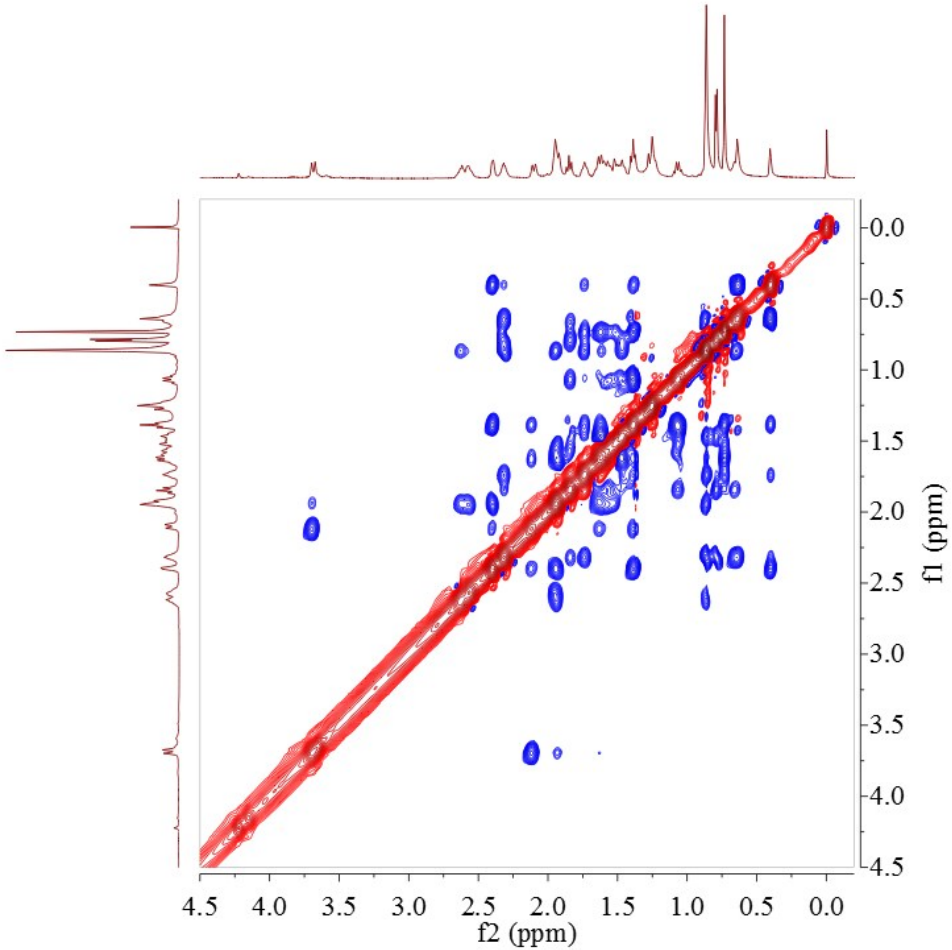

Fig. S26. ROESY spectrum of 3 in $CDCl_3$ at 600 MHz

Single Mass Analysis
Tolerance = 5.0 mDa / DBE: min = -1.5, max = 50.0
Element prediction: Off
Number of isotope peaks used for i-FIT = 3

Monoisotopic Mass, Even Electron Ions
92 formula(e) evaluated with 1 results within limits (up to 50 best isotopic matches for each mass)
Elements Used:
C: 0-100 H: 0-200 O: 0-100

3651-2
2018052930 264 (2.132)

1: TOF MS ES+
1.36e+006

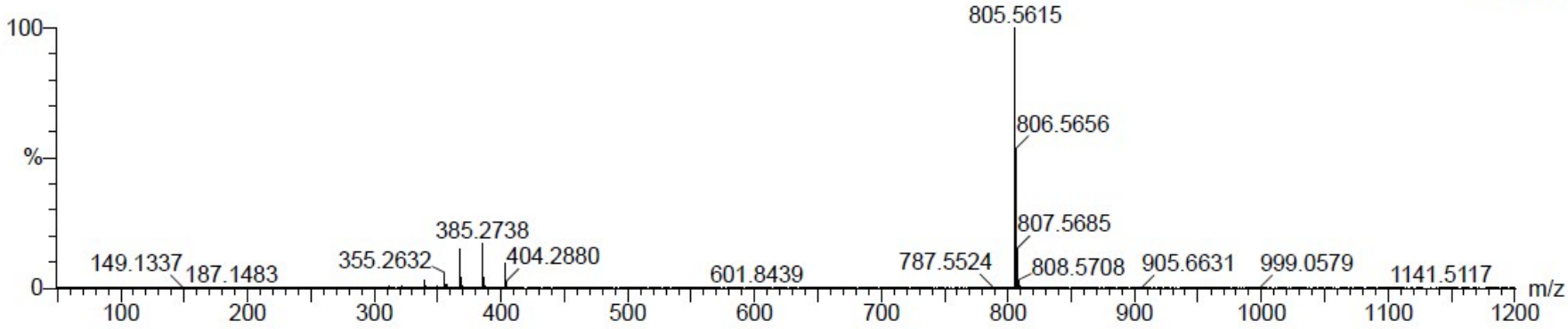

Minimum:				-1.5				
Maximum:		5.0	10.0	50.0				
Mass	Calc. Mass	mDa	PPM	DBE	i-FIT	Norm	Conf(%)	Formula
403.2847	403.2848	-0.1	-0.2	6.5	234.4	n/a	n/a	C25 H39 O4

Fig. S27. HRESIMS spectrum of 4

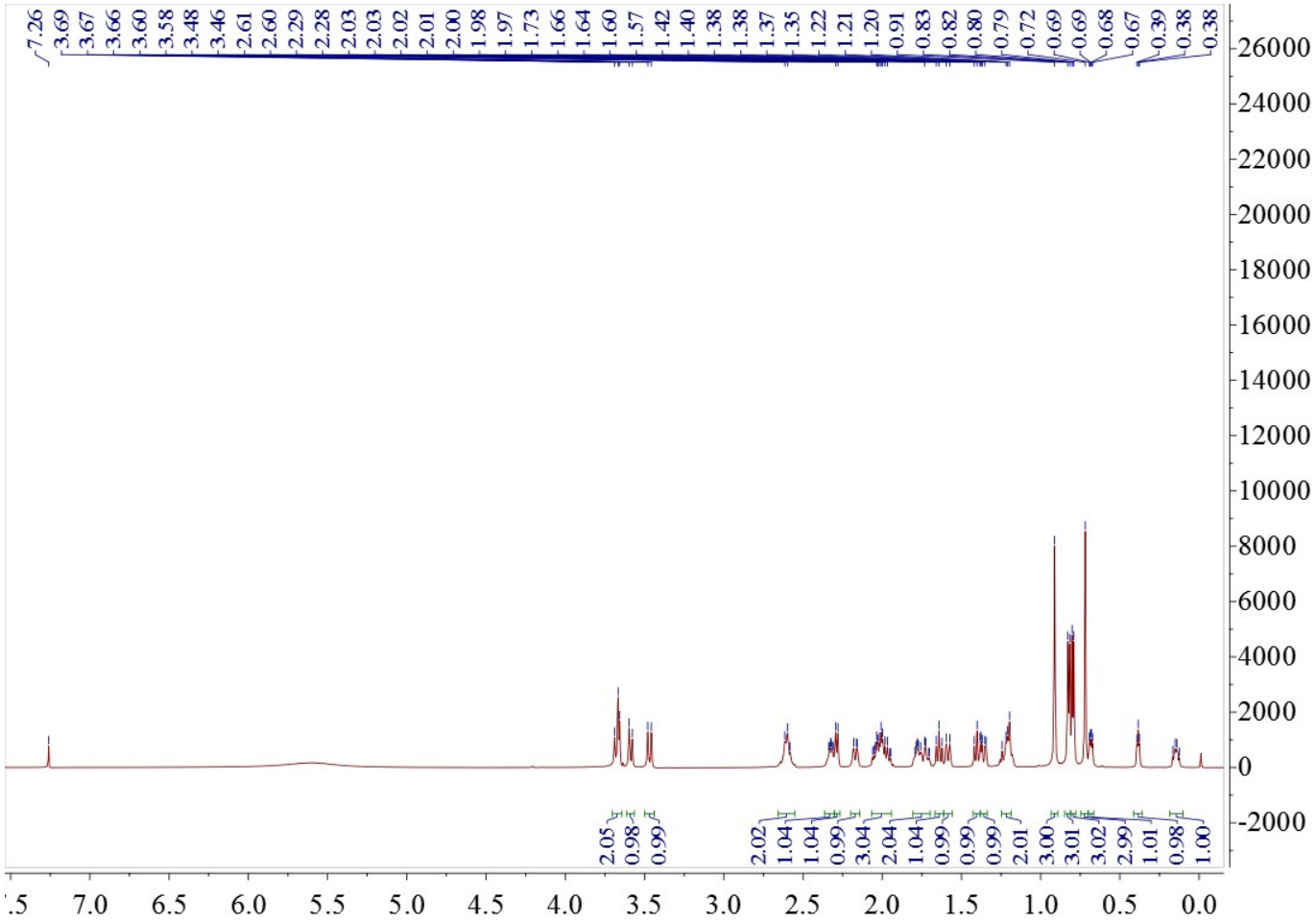

Fig. S28. ^{1}H NMR spectrum of 4 in $CDCl_3$ at 600 MHz

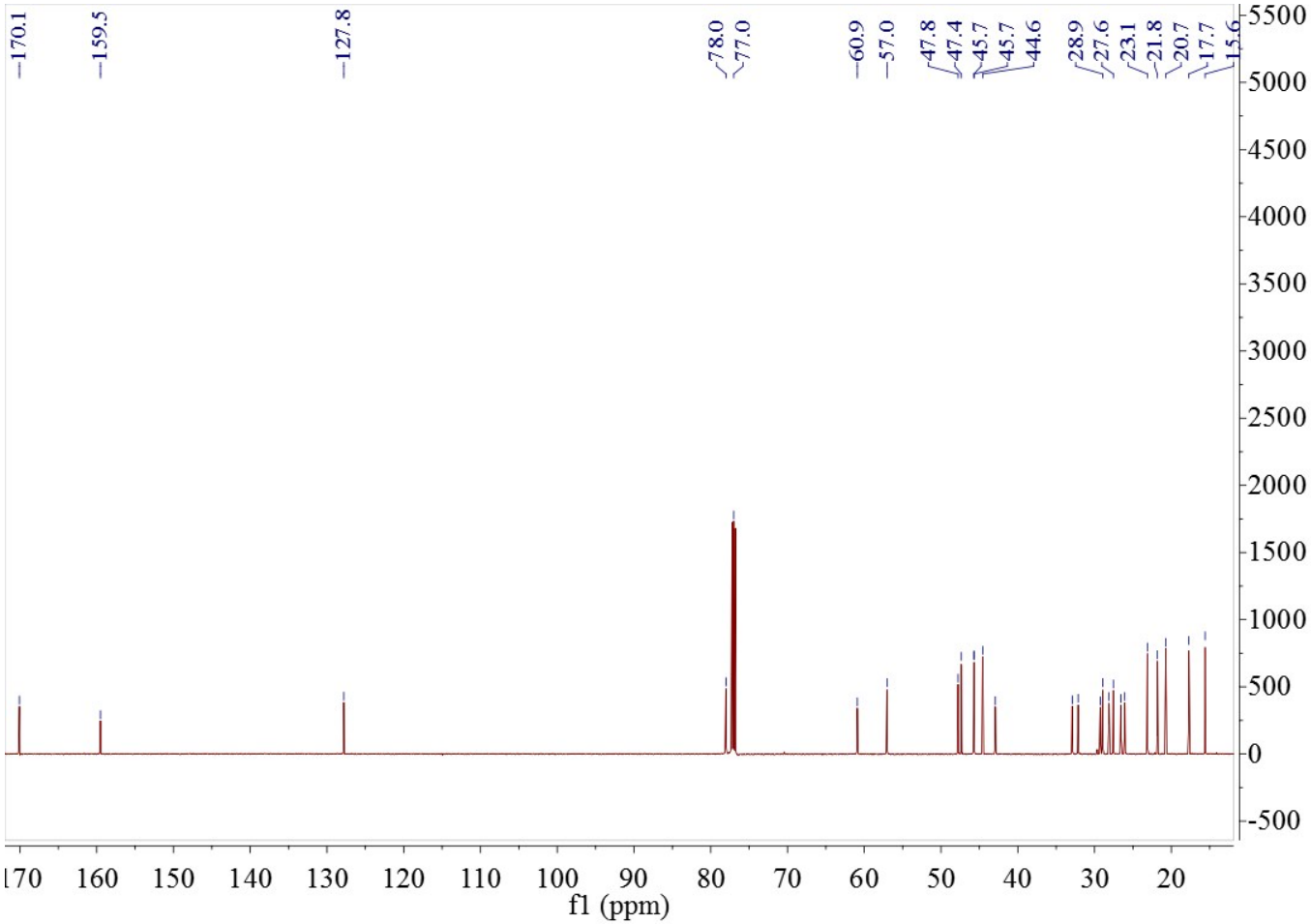

Fig. S29. ^{13}C NMR spectrum of 4 in $CDCl_3$ at 150 MHz

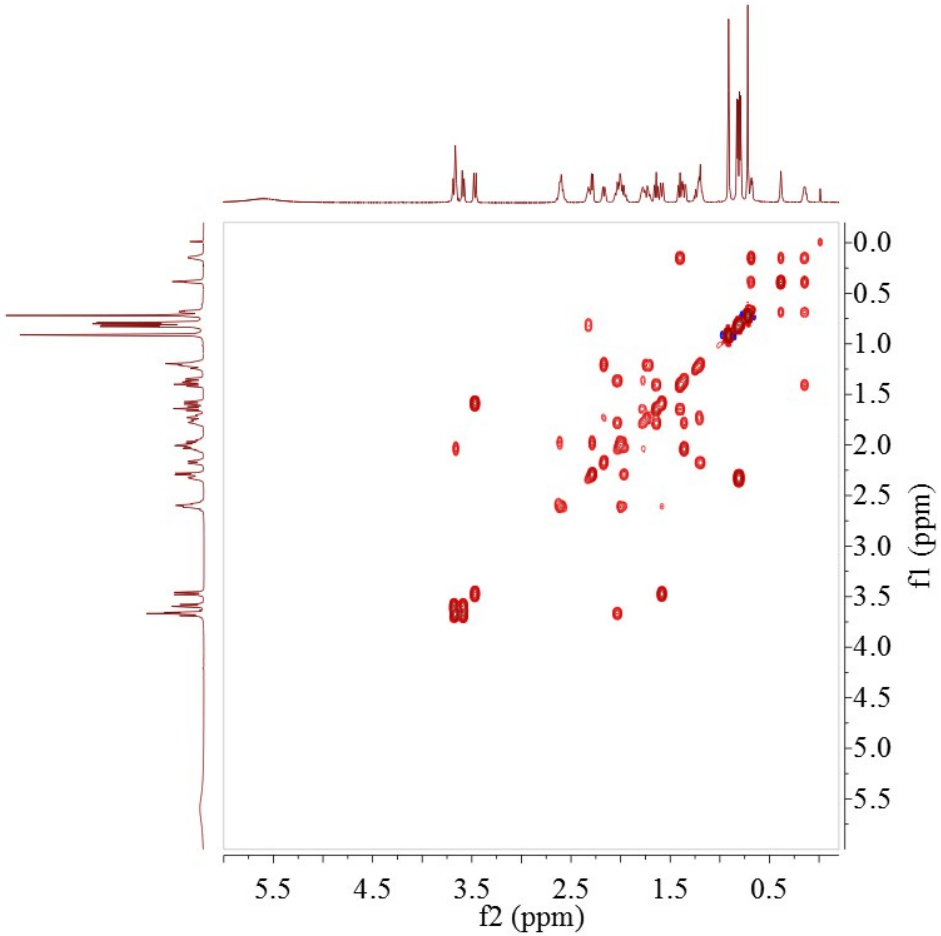

Fig. S30. ^{1}H-^{1}H COSY spectrum of 4 in $CDCl_3$ at 600 MHz

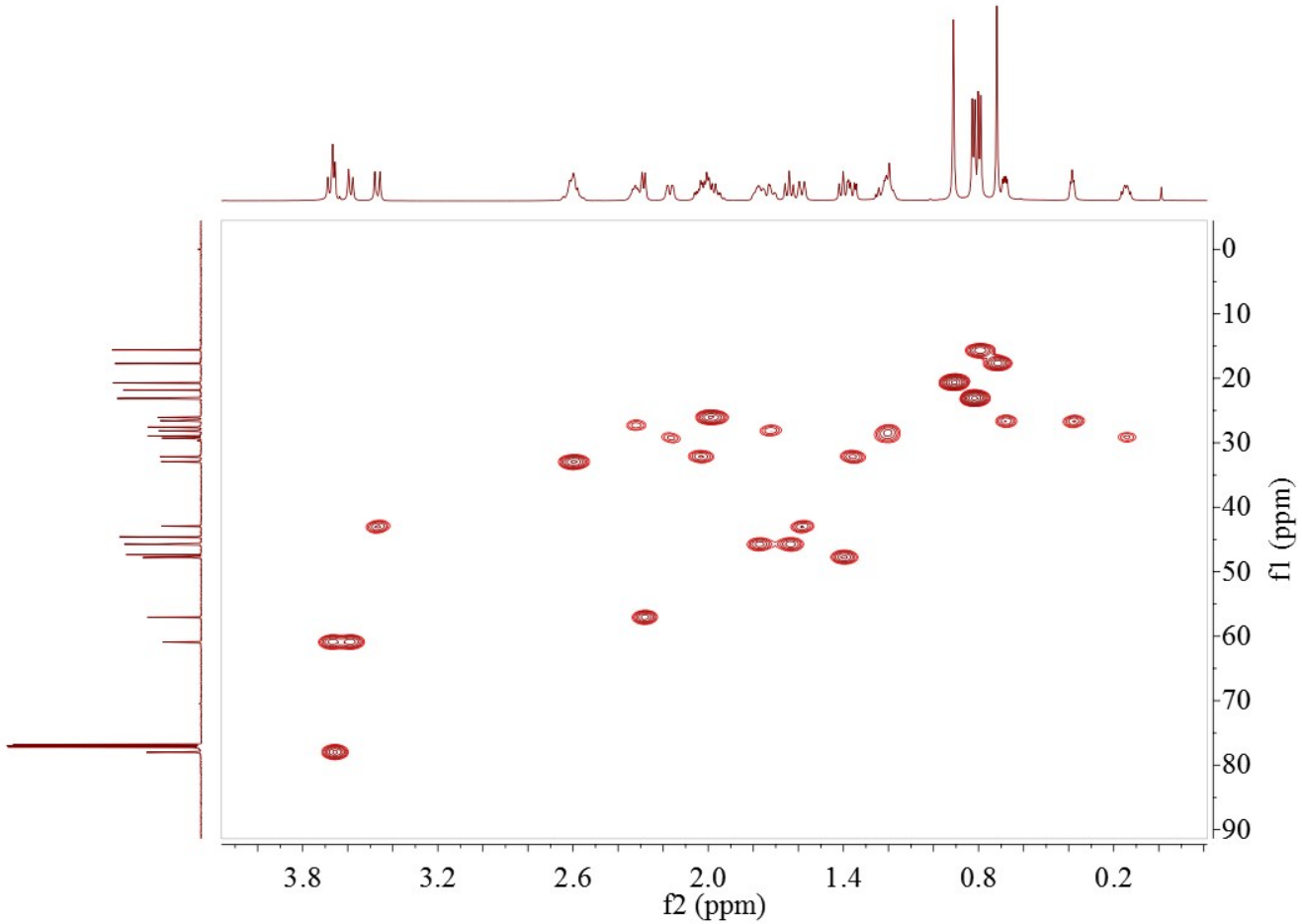

Fig. S31. HSQC spectrum of 4 in $CDCl_3$ at 600 MHz

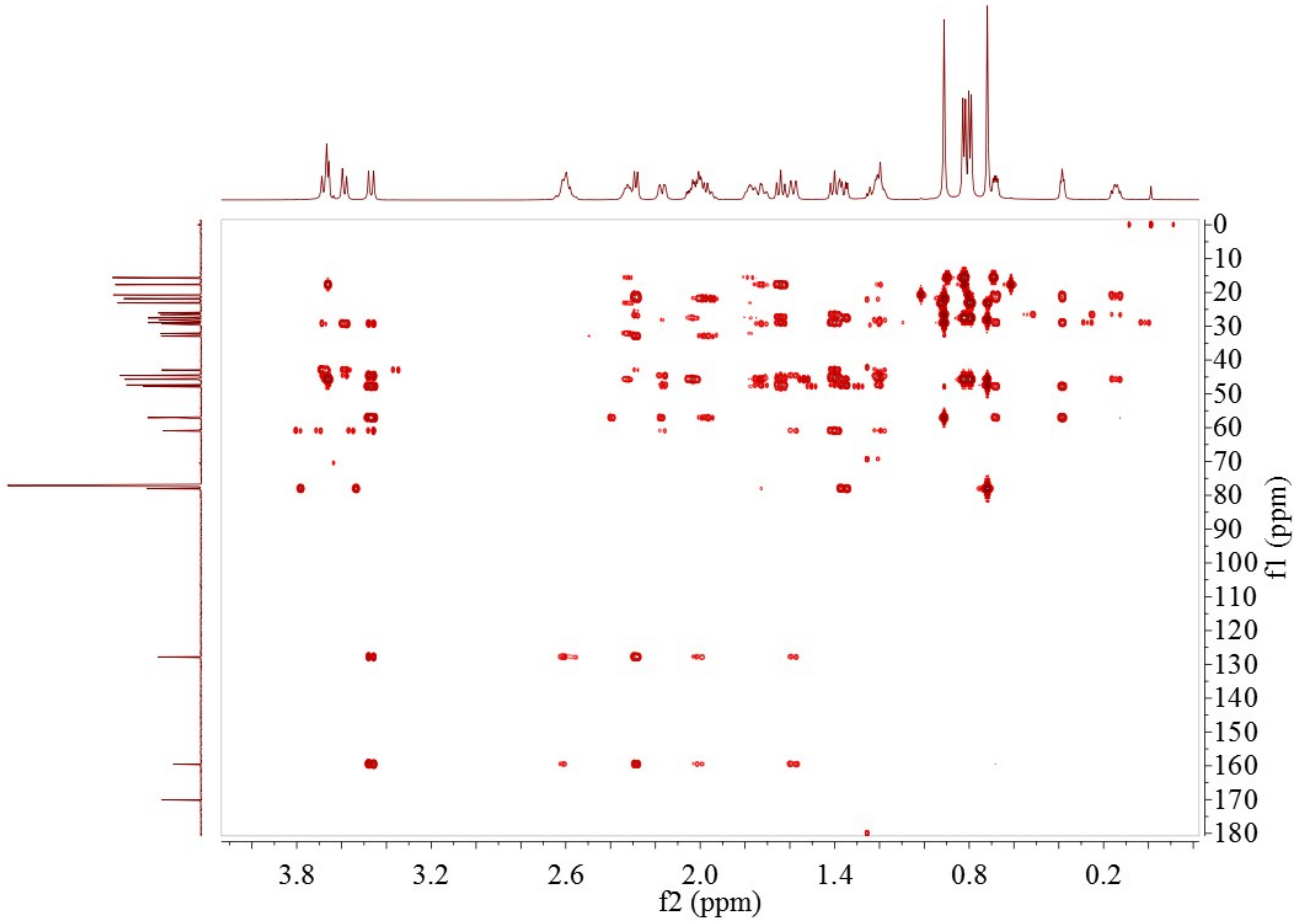

Fig. S32. HMBC spectrum of 4 in $CDCl_3$ at 600 MHz

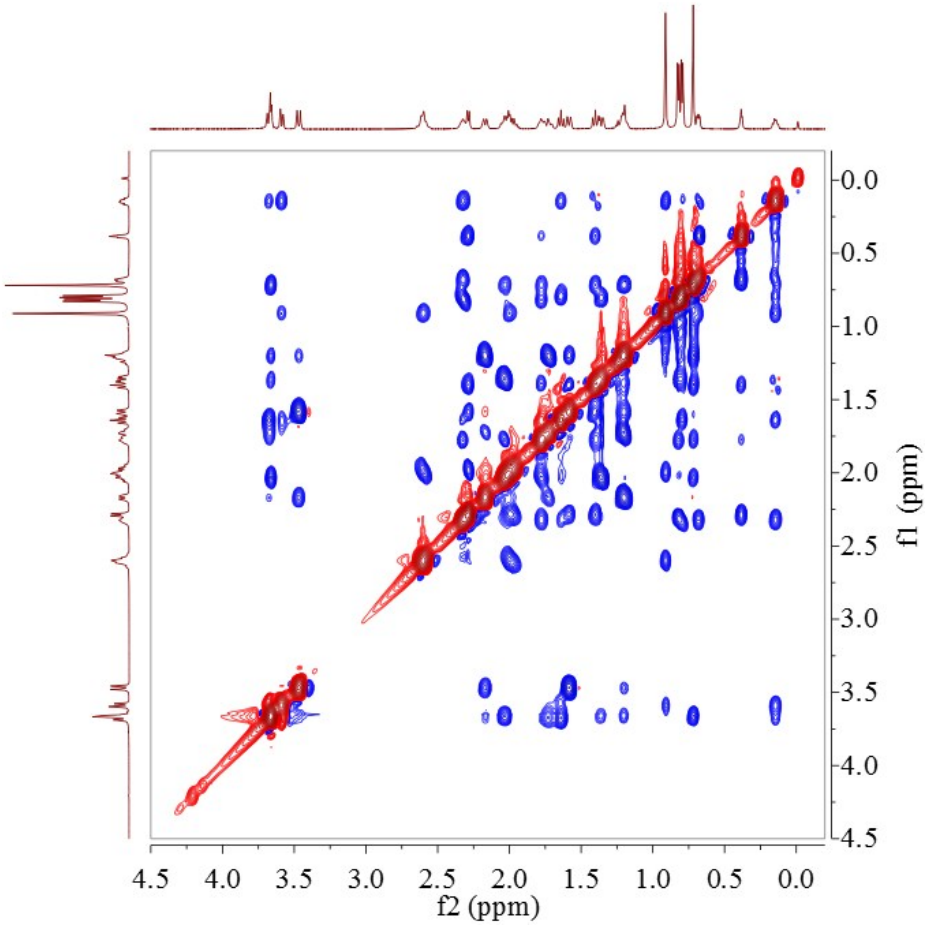

Fig. S33. ROESY spectrum of 4 in $CDCl_3$ at 600 MHz

Supplementary References

[1] Jin, F. J.; Maruyama, J.; Juvvadi, P. R.; Arioka, M.; Kitamoto, K. *FEMS Microbiol Lett* **2004,** *239*, 79-85.

[2] Frisch, M. J.; Trucks, G. W.; Schlegel, H. B.; Scuseria, G. E.; Robb, M. A.; Cheeseman, J. R.; Scalmani, G.; Barone, V.; Mennucci, B.; Petersson, G. A.; Nakatsuji, H.; Caricato, M.; Li, X.; Hratchian, H. P.; Izmaylov, A. F.; Bloino, J.; Zheng, G.; Sonnenberg, J. L.; Hada, M.; Ehara, M.; Toyota, K.; Fukuda, R.; Hasegawa, J.; Ishida, M.; Nakajima, T.; Honda, Y.; Kitao, O.; Nakai, H.; Vreven, T.; Montgomery, J. A., Jr.; Peralta, J. E.; Ogliaro, F.; Bearpark, M.; Heyd, J. J.; Brothers, E.; Kudin, K. N.; Staroverov, V. N.; Kobayashi, R.; Normand, J.; Raghavachari, K.; Rendell, A.; Burant, J. C.; Iyengar, S. S.; Tomasi, J.; Cossi, M.; Rega, N.; Millam, J. M.; Klene, M.; Knox, J. E.; Cross, J. B.; Bakken, V.; Adamo, C.; Jaramillo, J.; Gomperts, R.; Stratmann, R. E.; Yazyev, O.; Austin, A. J.; Cammi, R.; Pomelli, C.; Ochterski, J. W.; Martin, R. L.; Morokuma, K.; Zakrzewski, V. G.; Voth, G. A.; Salvador, P.; Dannenberg, J. J.; Dapprich, S.; Daniels, A. D.; Farkas, Ö.; Foresman, J. B.; Ortiz, J. V.; Cioslowski, J.; Fox, D. J. Gaussian 09, Revision C1; Gaussian, Inc., Wallingford CT, **2010**.

[3] Grimblat, N.; Zanardi, M. M.; Sarotti, A. M. *J Org Chem* **2013,** *25*, 243–249.

[4] Mitsuhashi, T.; Rinkel, J.; Okada, M.; Abe, I.; Dickschat, J. S. *Chem Eur J* **2017,** *23*, 10053-10057.

[5] Huang, X.; Huang, H.; Li, H.; Sun, X.; Huang, H.; Lu, Y.; Lin, Y.; Long, Y.; She, Z. *Org Lett* **2013,** *15*, 721-723.

[6] Fujii, T.; Yamaoka, H.; Gomi, K.; Kitamoto, K.; Kumaga, C. *Biosci Biotechnol Biochem* **1995,** *59*, 1869−1874.

[7] Jin F. J.; Maruyama, J.; Juvvadi, P. R.; Arioka, M.; Kitamoto, K. *Biosci Biotechnol Biochem* **2004,** *68*, 656-662.

[8] Narita, K.; Minami, A.; Ozaki, T.; Liu, C.; Kodama, M.; Oikawa, H. *J Org Chem* **2018,** *83*, 7042-7048.

[9] Narita, K.; Chiba, R.; Minami, A.; Kodama, M.; Fujii, I.; Gomi, K.; Oikawa, H. *Org Lett* **2016,** *18*, 1980-1983.

[10] Tokai, T.; Koshino, H.; Takahashi-Ando, N.; Sato, M.; Fujimura, M.; Kimura, M. *Biochem Biophys Res Commun* **2007,** *353*, 412-417.

[11] Lv, J. M.; Hu, D.; Gao, H.; Kushiro, T.; Awakawa, T.; Chen, G. D.; Wang, C. X.; Abe, I.; Yao, X. S. *Nat Commun* **2017,** *8*, 1644.

[12] Ishiuchi, K.; Nakazawa, T.; Yagishita, F.; Mino, T.; Noguchi, H.; Hotta, K.; Watanabe, K. *J Am Chem Soc* **2013,** *135*, 7371-7377.

[13] Fujii, R.; Minami, A.; Tsukagoshi, T.; Sato, N.; Sahara, T.; Ohgiya, S.; Gomi, K.; Oikawa, H. *Biosci Biotechnol Biochem* **2011,** *75*, 1813-1817.

[14] Matsuda, Y.; Quan, Z.; Mitsuhashi, T.; Li, C.; Abe, I. *Org Lett* **2016,** *18*, 296-299.

[15] Qiao, K.; Chooi, Y. H.; Tang, Y. *Metab Eng* **2011,** *13*, 723-732.